華南農業大學
South China Agricultural University

岩土工程大变形数值模拟的光滑粒子有限单元法

华南农业大学

水利与土木工程学院

张巍

目　录

研究背景

- 岩土工程领域经常涉及大变形问题
  - 滑坡、泥石流
  - 取样、原位试验、预制桩贯入

云南省镇雄赵家沟村(2013年，46人死亡)

浙江省丽水市(2015年，38人死亡)

- 12·20深圳山体滑坡(2015年，73人死亡)

研究背景

- 原位试验

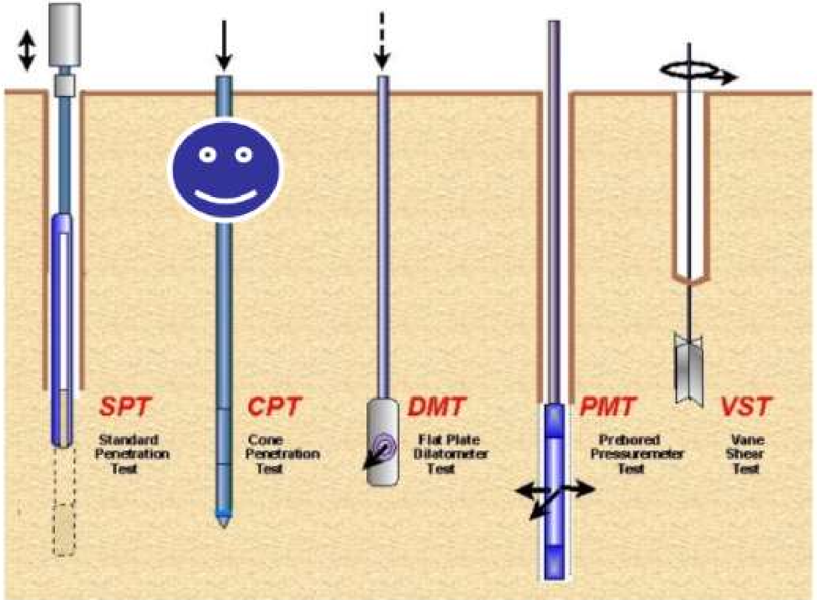

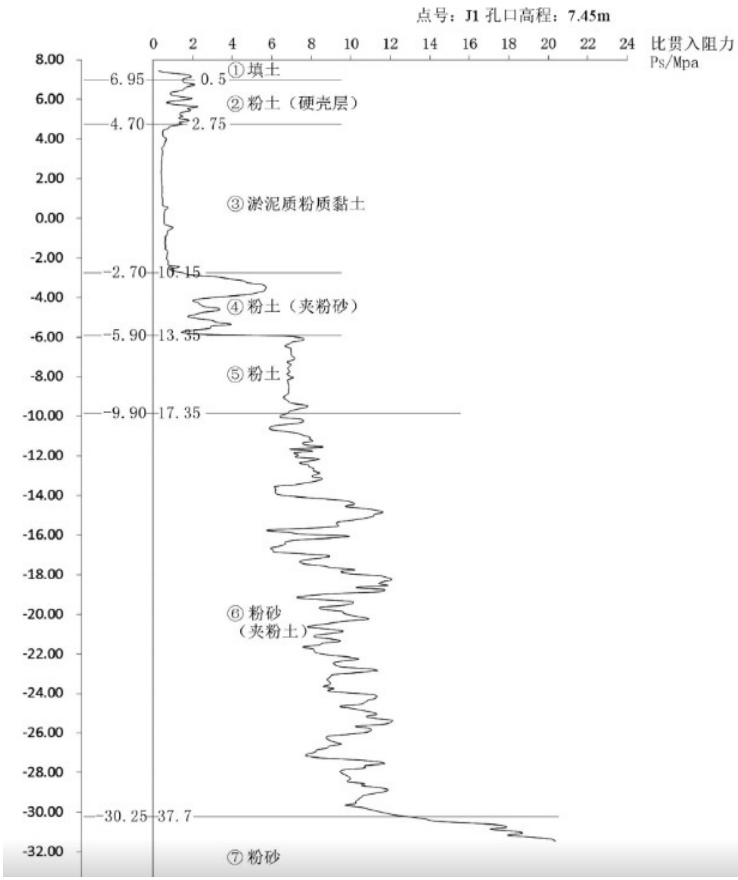

- 静力触探试验(CPT)

研究背景

- 预制桩贯入

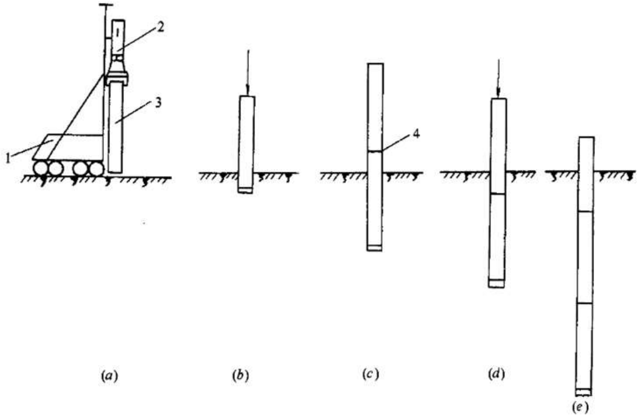

目　录

粒子有限元法(PFEM)

◻ Why PFEM (particle finite element method)?

We have a lot of numerical methods that can solve large deformation problems, i.e. ALE, SPH, CEL, MPM, PFEM ......

There are mainly two reasons:

- Easy to implement, it can be easy realized from FEM codes.
- It inherits the accuracy of FEM.

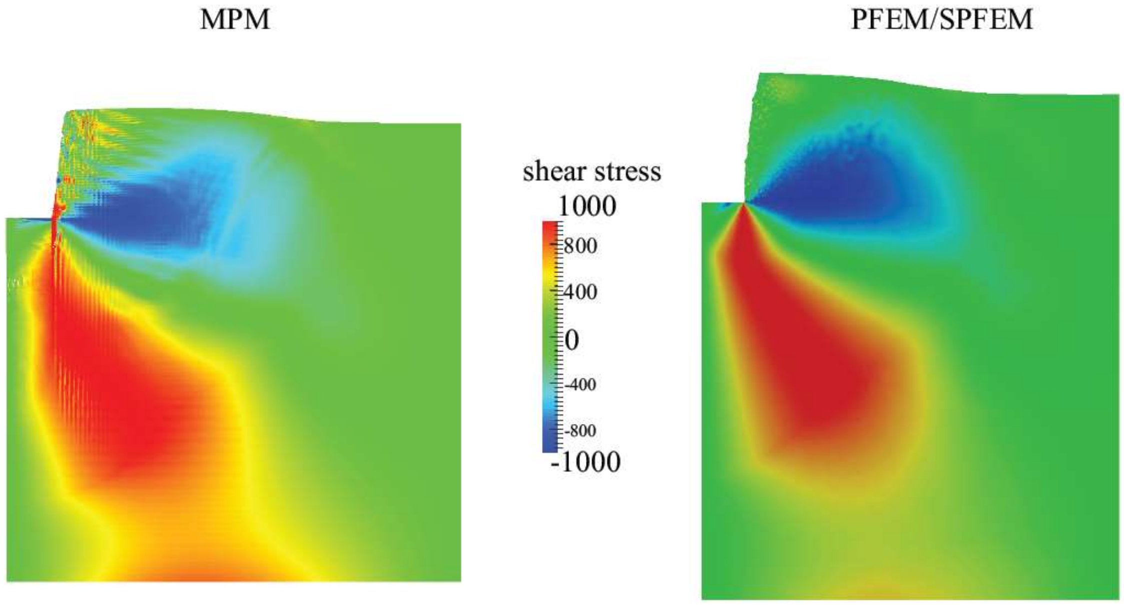

Footing penetration in Trescal soil

粒子有限元法(PFEM)

- PFEM applications:

Granular columns collapse

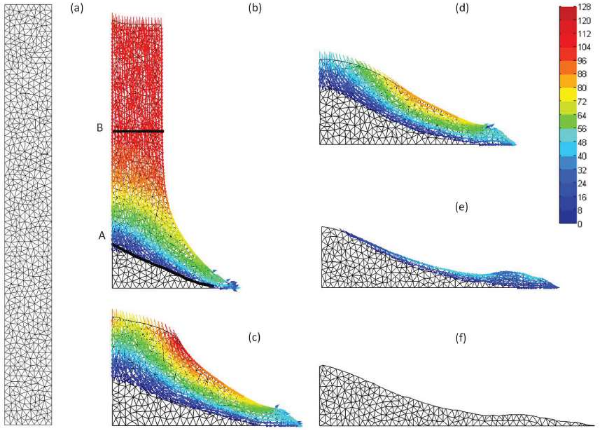

Cylinder soil interaction

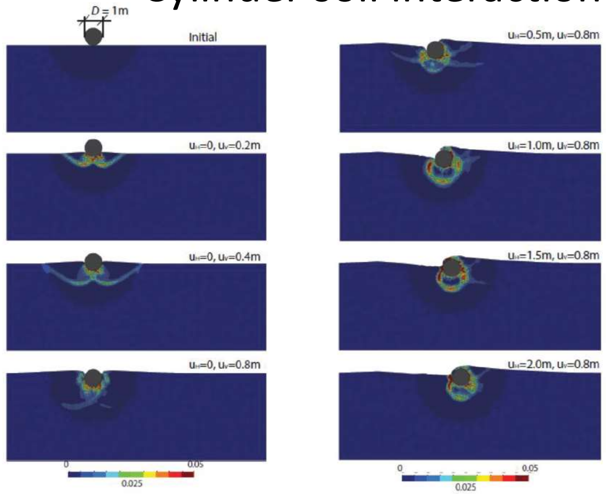

Progressive landslide

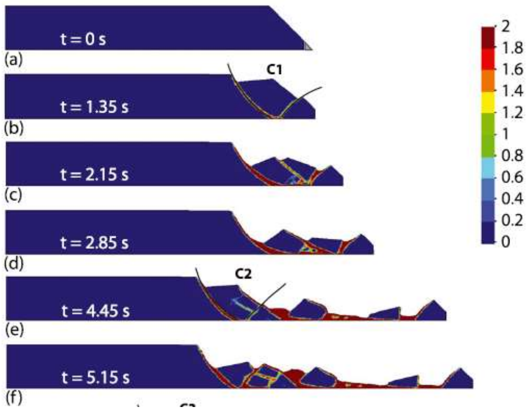

Cone penetration test

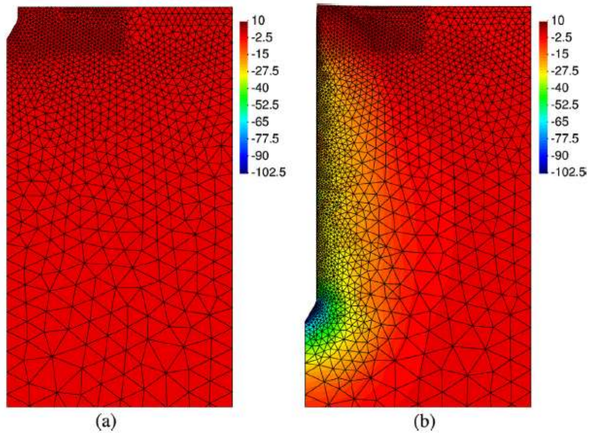

粒子有限元法(PFEM)

Typical step of PFEM:

1. On the basis of cloud of particles, the Delaunay triangulation technique is used to build the FEM mesh.
2. The alpha-shape approach is used to identify the entire problem domain.
3. Map the state variables (strain, stress, etc.) from particles to Gauss points.
4. Solve the governing equations via a standard incremental FEM approach.
5. Map the state variables (strain, stress, etc.) from the Gauss points to the particles
6. Modify the positions of particles and transfer all the field information of particles to form a new cloud of particles.
7. Go back to Step 1 and repeat until the problem-dependent stop condition.

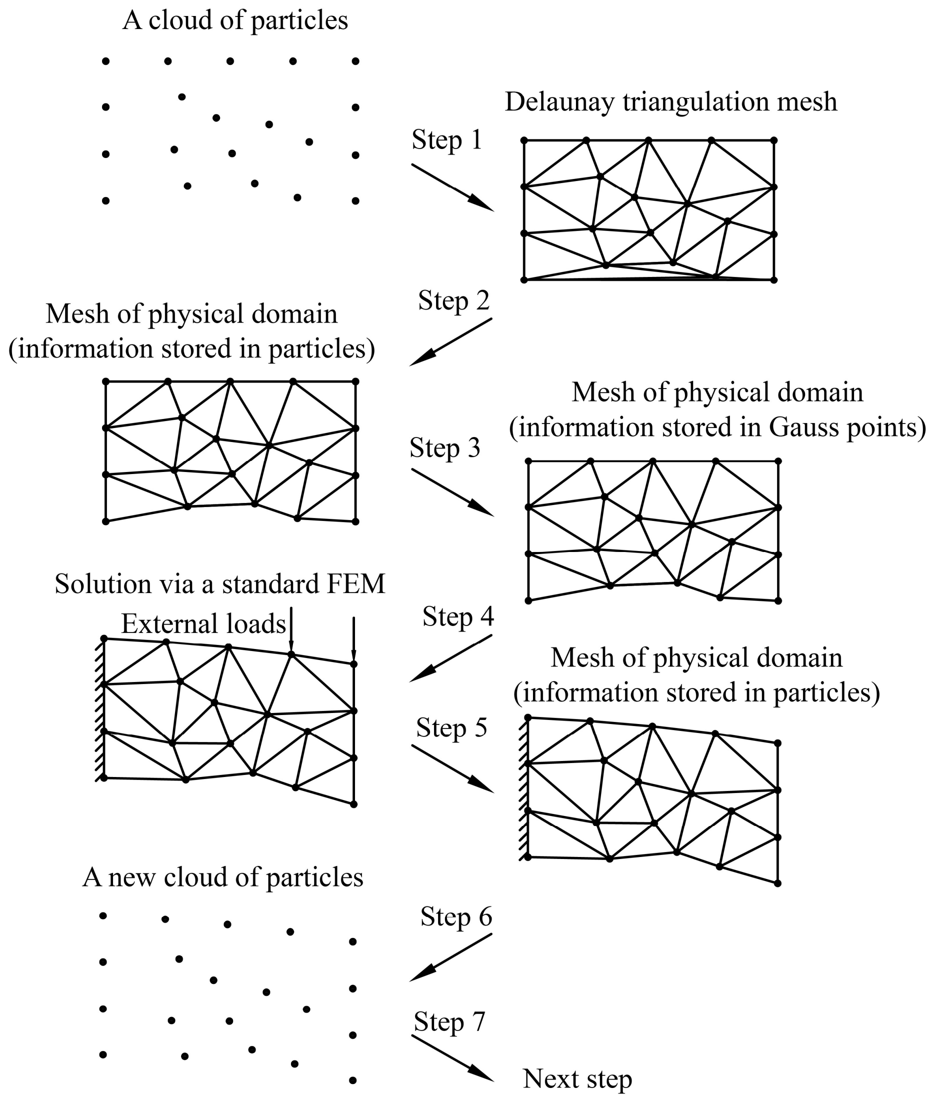

粒子有限元法(PFEM)

PFEM defects:

- Mapping induced errors due to the frequent information (e.g. stress, strain, plastic strain)
 transfer between old and new meshes.
- Volumetric locking due to the use of low order elements, and therefore 6-node elements are generally used.

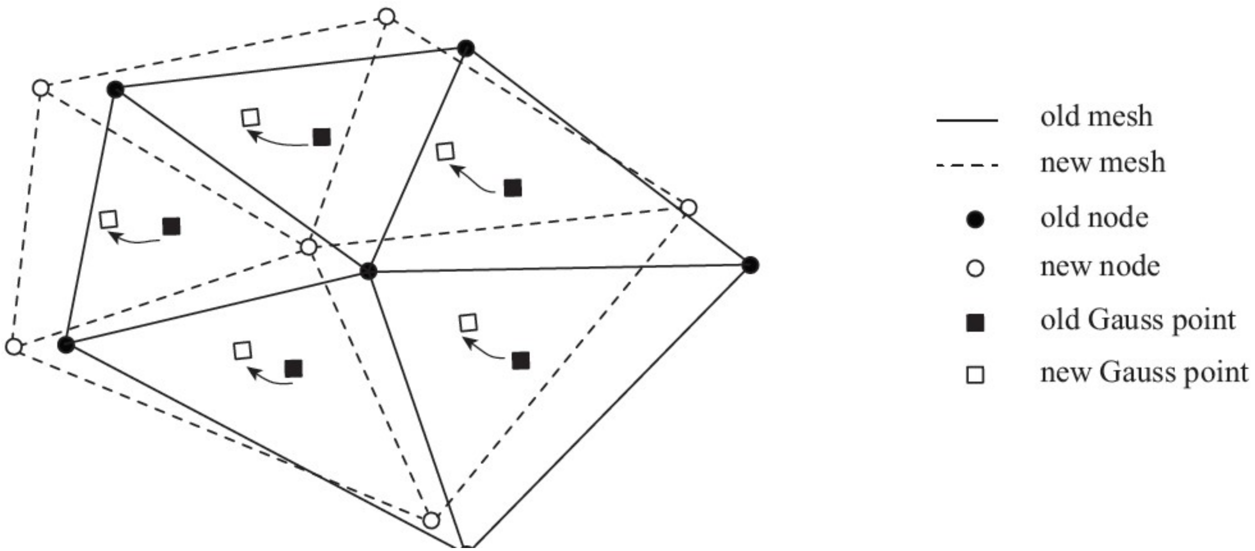

光滑粒子有限元法(PFEM)

Core of SPFEM:

Strain smoothing technique for nodal integration is incorporated.

Construction of strain smoothing cells associated with particles

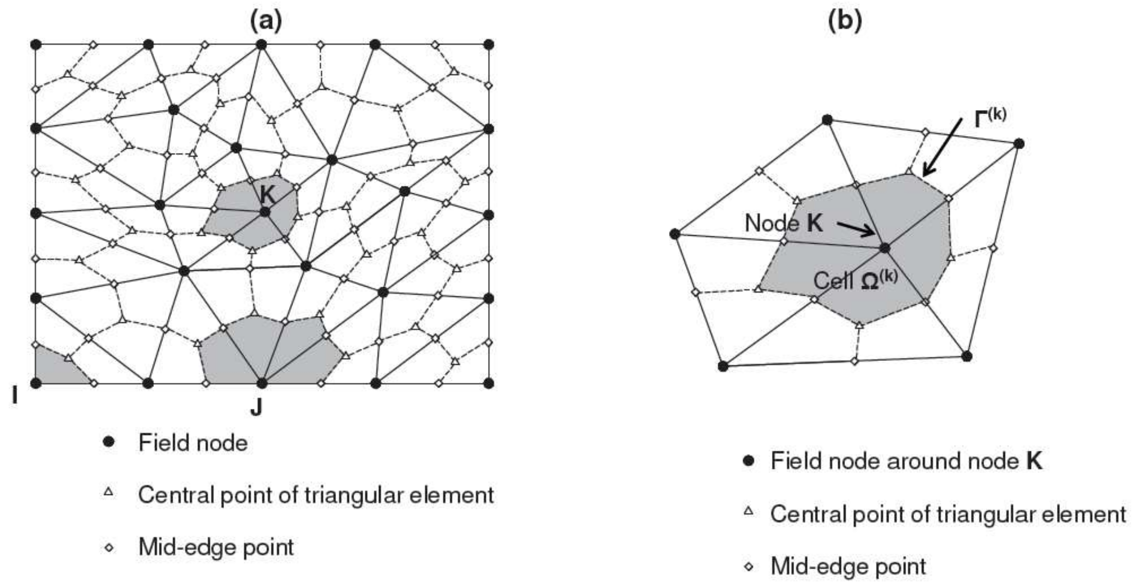

Details in:
Liu, G. R., Nguyen-Thoi, T., Nguyen-Xuan, H., and Lam, K. Y., 2009. A node-based smoothed finite element method (NS-FEM) for upper bound solutions to solid mechanics problems. Computers and Structures, 87(1-2), 14-26.

Chen, J. S., Wu, C. T., Yoon, S., and You, Y. (2001). "A stabilized conforming nodal integration for Galerkin mesh-free methods." Int. J. Numer.Methods Eng., 50(2), 435–466.

光滑粒子有限元法(PFEM)

Strain smoothing technique for SPFEM

The smoothed derivative of shape function for particle k at the h direction ($h = x, y$) can be obtained as follows:

$$\widetilde{b}_{Ih}(\boldsymbol{x}_k) = \frac{1}{A^{(k)}} \int_{\Gamma^{(k)}} N_I(\boldsymbol{x}) n_h(\boldsymbol{x}) d\Gamma$$

As the gradient of displacement is constant in each element (3-node triangular element), $\widetilde{b}_{Ih}(\boldsymbol{x}_{\boldsymbol{k}})$ can be further simplified and obtained as follows:

$$\widetilde{b}_{Ih}(\boldsymbol{x}_k) = \frac{1}{A^{(k)}} \sum_{j=1}^{N_e^{(k)}} \frac{1}{3} A_e^j N_{I,h}^j$$

where A_e^j and $N_{I,h}$ are the area and derivative of shape function for the jth triangular element around the particle k, respectively.

光滑粒子有限元法(PFEM)

Strain smoothing technique for SPFEM

The area of the smoothing cell $A^{(k)}$ is obtained as follows:

$$A^{(k)} = \int_{\Omega^{(k)}} d\Omega = \frac{1}{3} \sum_{j=1}^{N_e^{(k)}} A_e^j$$

The smoothed strain-displacement operators $\widetilde{B}$ at the Ith node can be obtained as follows:

$$\widetilde{\boldsymbol{B}}_L = \begin{bmatrix} \widetilde{b}_{Ix} & 0 \\ 0 & \widetilde{b}_{Iy} \\ \widetilde{b}_{Iy} & \widetilde{b}_{Ix} \end{bmatrix}$$

光滑粒子有限元法(PFEM)

- Typical step of SPFEM:

Due to this special technique, Step 3 and Step 5 vanishes in the original PFEM.

1. On the basis of cloud of particles, the Delaunay triangulation technique is used to build the FEM mesh.
2. The alpha-shape approach is used to identify the entire problem domain.
3. ~~Map the state variables (strain, stress, etc.) from particles to Gauss points.~~
4. Solve the governing equations via a standard incremental FEM approach.
5. ~~Map the state variables (strain, stress, etc.) from the Gauss points to the particles~~
6. Modify the positions of particles and transfer all the field information of particles to form a new cloud of particles.
7. Go back to Step 1 and repeat until the problem-dependent stop condition.

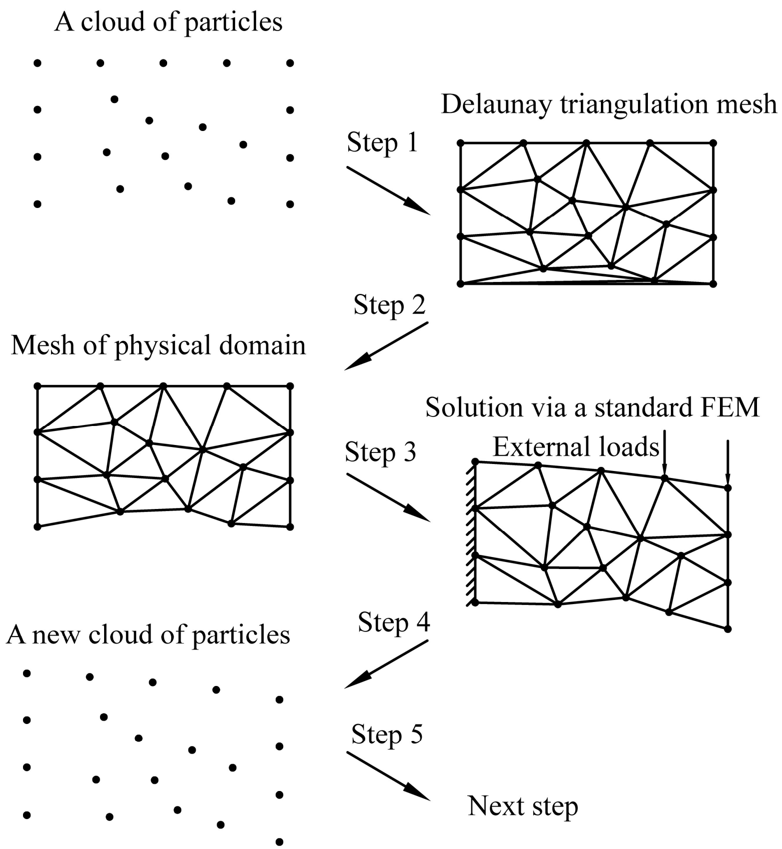

光滑粒子有限元法(PFEM)

与传统的PFEM相比，光滑粒子有限元法SPFEM有如下优点：

- 更像基于粒子的计算方法
- 避免了高斯点与节点之间的信息映射
- 使用低阶单元但没有体积锁定
- 对畸形单元不敏感

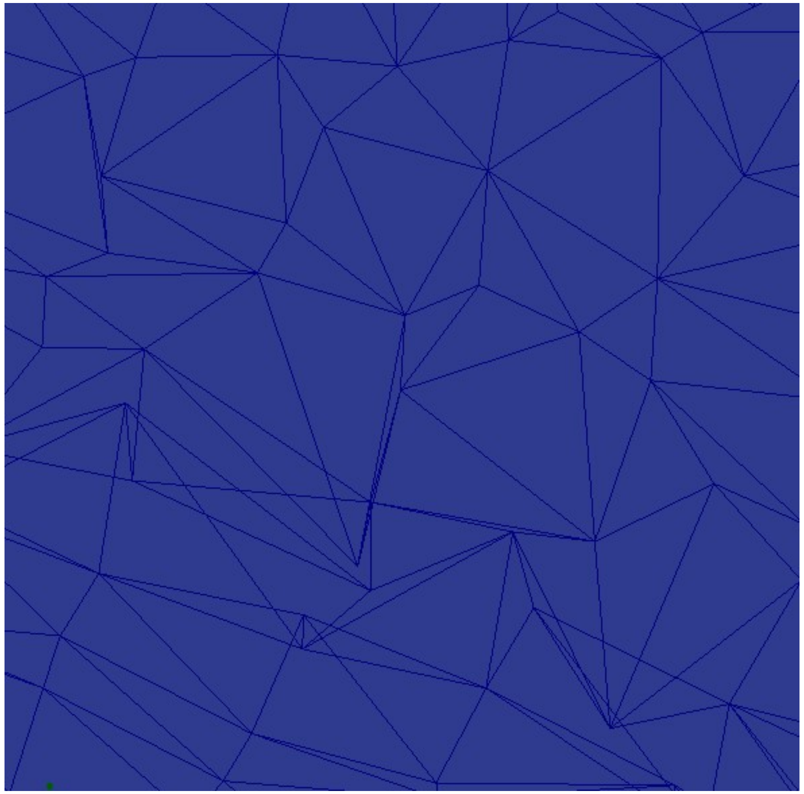

目　录

Implicit SPFEM

Similar to FEM and MPM, there are two types of SPFEM.

SPFEM
- Implicit SPFEM (Zhang, 2018)
- Explicit SPFEM (Yuan, 2019)

$$(\mathbf{K}_{\mathrm{ep}} + \mathbf{K}_{g})\mathbf{u} = \mathbf{F}^{\mathrm{ext}}$$

Implicit SPFEM

$$\boldsymbol{M}\boldsymbol{a} = \boldsymbol{F}^{ext} - \boldsymbol{F}^{int}$$

Explicit SPFEM

1. **Zhang W**, Yuan W, Dai B. A smoothed particle finite element method for large-deformation problems in geomechanics, International Journal of Geomechanics, 2018, 18(4): 04018010
2. Yuan W H, Wang B, **Zhang W**, et al. Development of an explicit smoothed particle finite element method for geotechnical applications[J]. Computers and Geotechnics, 2019, 106: 42-51.

Implicit SPFEM

1. Governing equation

$$\rho \boldsymbol{a} = \nabla \cdot \boldsymbol{\sigma} + \rho \boldsymbol{b}$$

2. Weak form

$$\int_{V^t} \mathbf{D}_{\mathrm{ep}} \cdot d\boldsymbol{\varepsilon} \cdot \delta \boldsymbol{\varepsilon} dV^t + \int_{V^t} \left(d\boldsymbol{\Omega} \cdot \boldsymbol{\sigma}^t + \boldsymbol{\sigma}^t \cdot d\boldsymbol{\Omega}^T \right) \cdot \delta \boldsymbol{\varepsilon} dV^t + \int_{V^t} \boldsymbol{\sigma}^{\mathrm{t}}$$

$$\cdot \delta \boldsymbol{\eta} dV^t = \int_{V^t} \mathbf{b}^{t+\Delta t} \cdot \delta \mathbf{u} dV^t + \int_{S^t} \mathbf{t}^{t+\Delta t} \cdot \delta \mathbf{u} dS^t - \int_{V^t} \boldsymbol{\sigma}^t \cdot \delta \boldsymbol{\varepsilon} dV^t$$

3. discretization formulations

$$(\mathbf{K}_{\mathrm{ep}} + \mathbf{K}_g)\mathbf{u} = \mathbf{F}^{\mathrm{ext}}$$

4. Newton-Raphson iteration

$$d\mathbf{u}_j = (\mathbf{K}_{j-1})^{-1}\mathbf{R}_{j-1}$$

$$\Delta\mathbf{u}_j = \Delta\mathbf{u}_{j-1} + d\mathbf{u}_j$$

$$\mathbf{u}_j^{t+\Delta t} = \mathbf{u}^t + \Delta\mathbf{u}_{\mathbf{j}}$$

Implicit SPFEM

3. discretization formulations

$$(\mathbf{K}_{\text{ep}} + \mathbf{K}_g)\mathbf{u} = \mathbf{F}^{\text{ext}} \qquad \mathbf{R}_{j-1} = \mathbf{F}^{\text{ext}} - \mathbf{F}^{\text{int}}$$

$$\mathbf{K}_{\text{ep}} = \int_\Omega \mathbf{B}_L^T \mathbf{D}_{\text{ep}} \mathbf{B}_L dV$$

$$\mathbf{K}_g = \int_\Omega \mathbf{B}_L^T \bar{\boldsymbol{\sigma}} \mathbf{B}_S dV + \int_\Omega \mathbf{B}_{\text{NL}}^T \hat{\boldsymbol{\sigma}} \mathbf{B}_{\text{NL}} dV$$

$$\mathbf{F}^{\text{int}} = \int_\Omega \mathbf{B}_L^T \boldsymbol{\sigma} dV$$

Traditional FEM

$$\mathbf{K}_{\text{ep}} = \sum_{k-1}^{N_n} \tilde{\mathbf{B}}_L^{(k)T} \mathbf{D}_{\text{ep}}^{(k)} \tilde{\mathbf{B}}_L^{(k)} A^{(k)}$$

$$\mathbf{K}_g = \sum_{k-1}^{N_n} \tilde{\mathbf{B}}_L^{(k)T} \bar{\boldsymbol{\sigma}}_k \tilde{\mathbf{B}}_S^{(k)} A^{(k)} + \sum_{k-1}^{N_n} \tilde{\mathbf{B}}_{\text{NL}}^{(k)T} \hat{\boldsymbol{\sigma}}_k \tilde{\mathbf{B}}_{\text{NL}}^{(k)} A^{(k)}$$

$$\mathbf{F}^{\text{int}} = \sum_{k-1}^{N_n} \tilde{\mathbf{B}}_L^{(k)T} \boldsymbol{\sigma}_k A^{(k)}$$

Nodal integration

Numerical procedure of iSPFEM

1. Read the particle information of the problem domain.
2. Loop over the load increment steps.
3. Generate the Delaunay triangles and identify the computational domain.
4. Construct the strain smoothing cells and compute the smoothed strain-displacement operators of all particles.
5. Solve the nonlinear equilibrium equations by the Newton-Raphson iteration to obtain particle incremental solutions of the current load incremental step.
6. Update the positions and field variables of particles.
7. End looping over the load increment steps.
8. Output results.

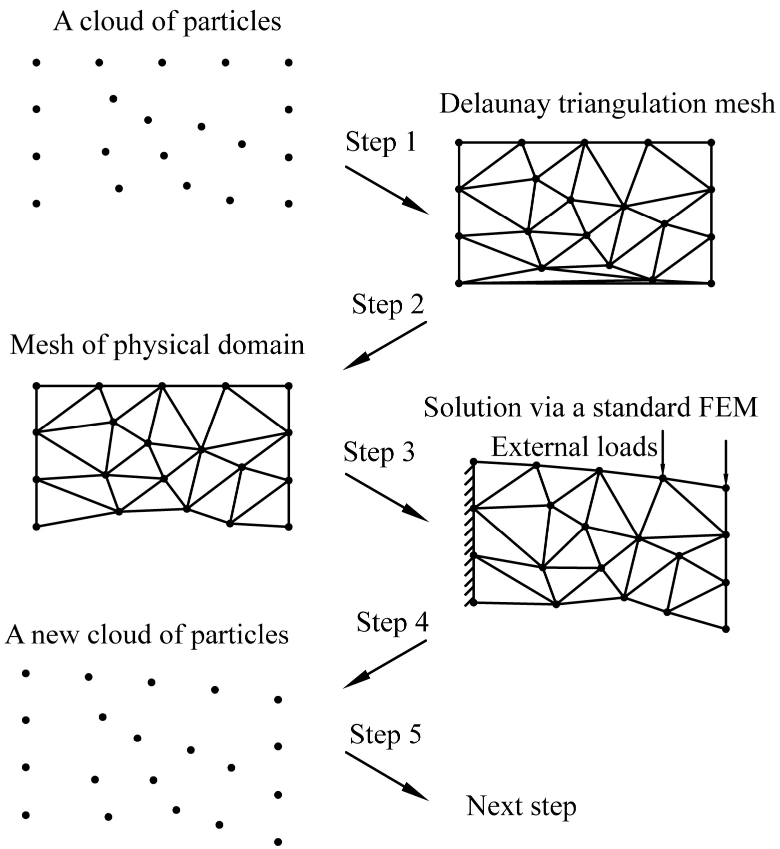

Explicit SPFEM

1. Governing equation

$$\rho \boldsymbol{a} = \nabla \cdot \boldsymbol{\sigma} + \rho \boldsymbol{b}$$

2. Weak form

$$\int_V \delta \boldsymbol{u} \cdot \rho \boldsymbol{a} dV = -\int_V \delta \boldsymbol{u} : \boldsymbol{\sigma} dV + \int_S \delta \boldsymbol{u} \cdot \boldsymbol{\tau}_S dS + \int_V \delta \boldsymbol{u} \cdot \rho \boldsymbol{b} dV$$

3. discretization formulations

$$\boldsymbol{M}\boldsymbol{a} = \boldsymbol{F}^{ext} - \boldsymbol{F}^{int}$$

$$\boxed{\boldsymbol{F}^{int} = \int_\Omega \tilde{\boldsymbol{B}}^T \boldsymbol{\sigma} d\Omega = \sum_{k=1}^{T} \sum_{i=1}^{N_k} \tilde{\boldsymbol{B}}_k^T \boldsymbol{\sigma}_k V_k}$$

Nodal integration

Computational cycle of eSPFEM

Algorithm 1 Computational cycle of SPFEM

1. Generate Mesh using Delaunay triangulation and alpha shape technique
2. Get indices of elements related to nodes.
3. Calculate incremental time step and volumes of elements and nodes
4. Calculate smoothed strains of nodes
5. Calculate stresses of nodes through constitutive integration
6. Calculate internal force of nodes
7. Update positions and velocities of nodes by explicit time integration

3. $$\Delta t_{cr} = \alpha \frac{l_{\min}}{c}$$

4. $$\tilde{\boldsymbol{B}}_k = \frac{1}{V_k} \sum_{i=1}^{N_k} \frac{1}{4} V^i \boldsymbol{B}^i$$

5. $$\dot{\boldsymbol{\sigma}} = H(\dot{\boldsymbol{\epsilon}}, \kappa)$$

6. $$\boldsymbol{F}^{int} = \int_{\Omega} \tilde{\boldsymbol{B}}^T \boldsymbol{\sigma} d\Omega = \sum_{k=1}^{T} \sum_{i=1}^{N_k} \tilde{\boldsymbol{B}}_k^T \boldsymbol{\sigma}_k V_k$$

7. $$\boldsymbol{M}\boldsymbol{a} = \boldsymbol{F}^{ext} - \boldsymbol{F}^{int}$$

The concise computaional cycle greatly facilitate the GPU parallel computation

Extension to 3D and GPU parallel computation

1. Construct strain smoothing cells
2. Calculate the smoothed strain

2D case:

$$\boldsymbol{A}_k = \sum_{i=1}^{N_k} \frac{1}{3} A^i$$

$$\tilde{\boldsymbol{B}}_k = \frac{1}{A_k} \sum_{i=1}^{N_k} \frac{1}{3} A^i \boldsymbol{B}^i$$

3D case:

$$\boldsymbol{V}_k = \sum_{i=1}^{N_k} \frac{1}{4} V^i$$

$$\tilde{\boldsymbol{B}}_k = \frac{1}{V_k} \sum_{i=1}^{N_k} \frac{1}{4} V^i \boldsymbol{B}^i$$

The geometric data of smoothing cells are not requried to be obtain explicitly.

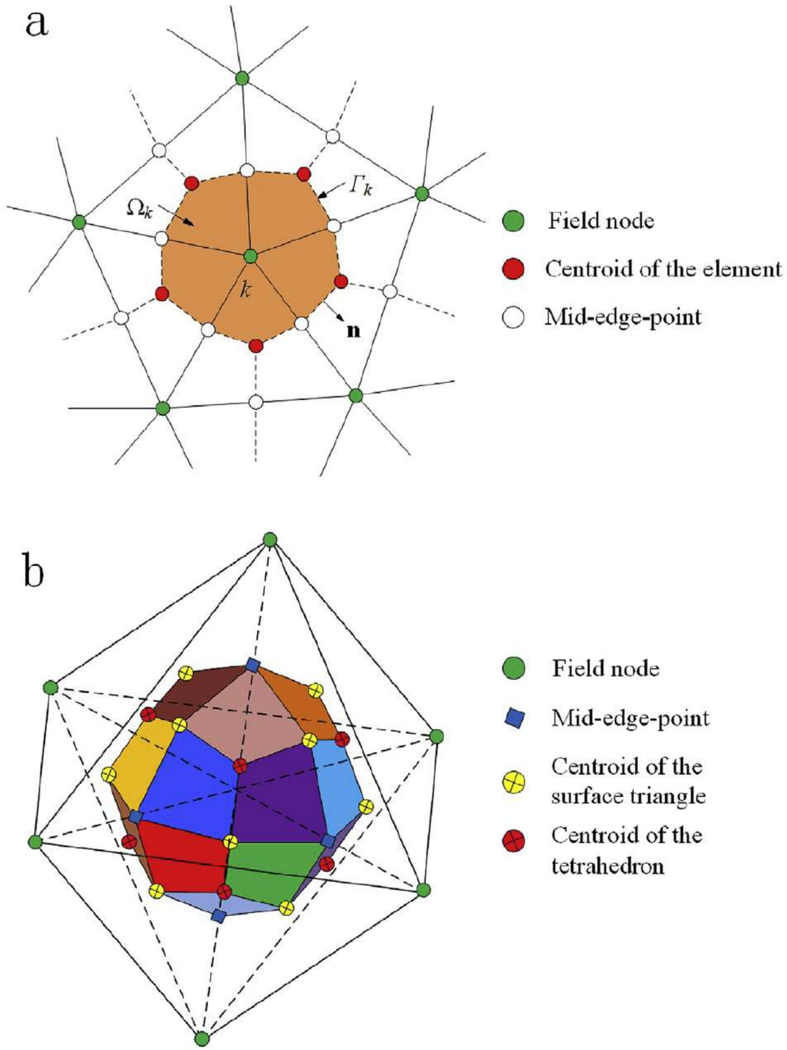

(Cui, 2016)

Step 6. Calculate internal force of nodes

$$\boldsymbol{F}^{int} = \int_{\Omega} \tilde{\boldsymbol{B}}^T \boldsymbol{\sigma} d\Omega = \sum_{k=1}^{T} \sum_{i=1}^{N_k} \tilde{\boldsymbol{B}}_k^T \boldsymbol{\sigma}_k V_k$$

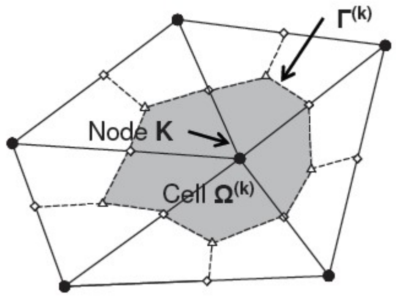

$$\tilde{\boldsymbol{B}}_k = \frac{1}{V_k} \sum_{i=1}^{N_k} \frac{1}{4} V^i \boldsymbol{B}^i$$

$$\boldsymbol{F}^{int} = \sum_{k=1}^{T} \sum_{i=1}^{N_k} \sum_{j=1}^{E_k} \frac{1}{4} V^j \boldsymbol{B}^j \boldsymbol{\sigma}_k = \sum_{k=1}^{T} \sum_{j=1}^{E_k} \sum_{m=1}^{4} \frac{1}{4} V^j \boldsymbol{B}_m^j \boldsymbol{\sigma}_k$$

Smoothing strain matrices are too large! ($T \times N_k \times 18$)

- ✓ To save global memory, we reformulate the calculation of internal force.
- ✓ Atomic operations are used to avoid racing conditions.

Parallelisation schemes for the eSPFEM

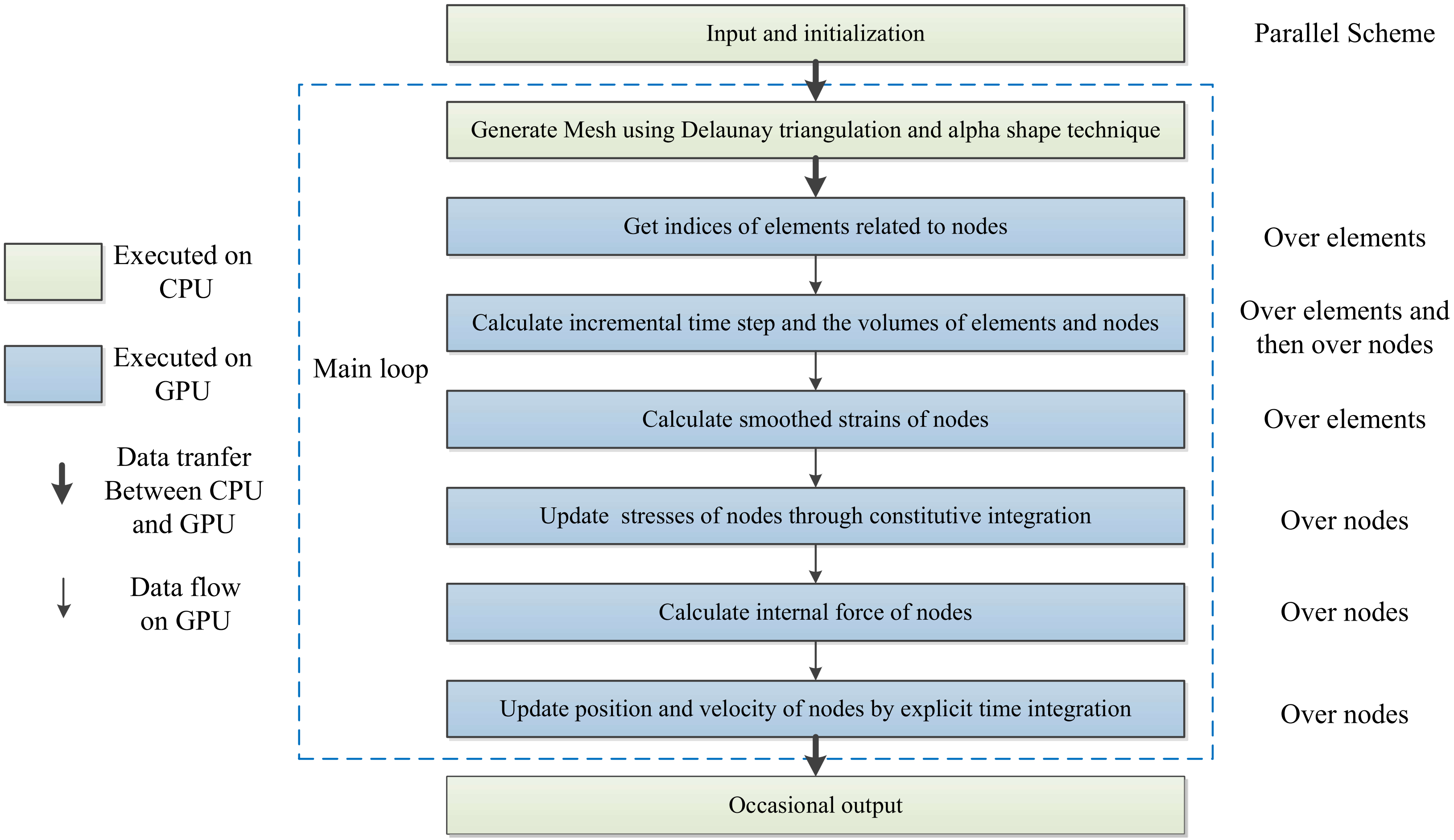

Zhang W, Zhong Z, Peng C, et al. GPU-accelerated smoothed particle finite element method for large deformation analysis in geomechanics. Computers & Geotechnics, 2021, doi: 10.1016/j.compgeo.2020.103856

PFEM for large deformation consolidation analysis

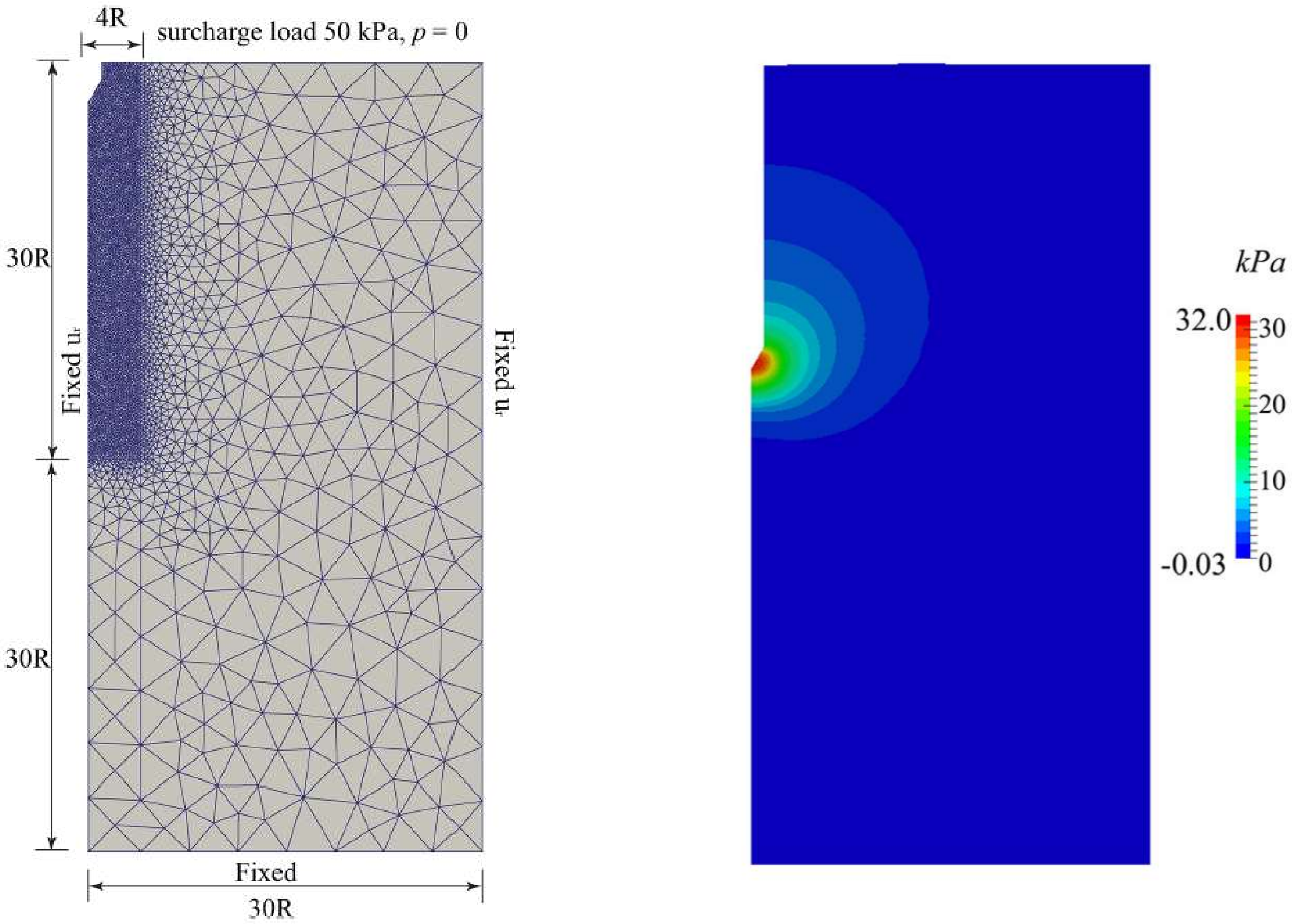

Yuan W, **Zhang W**(*), Dai B, Application of the particle finite element method for large deformation consolidation analysis, Engineering Computations, 2019, 36(9): 3138-3163

PFEM with Abaqus

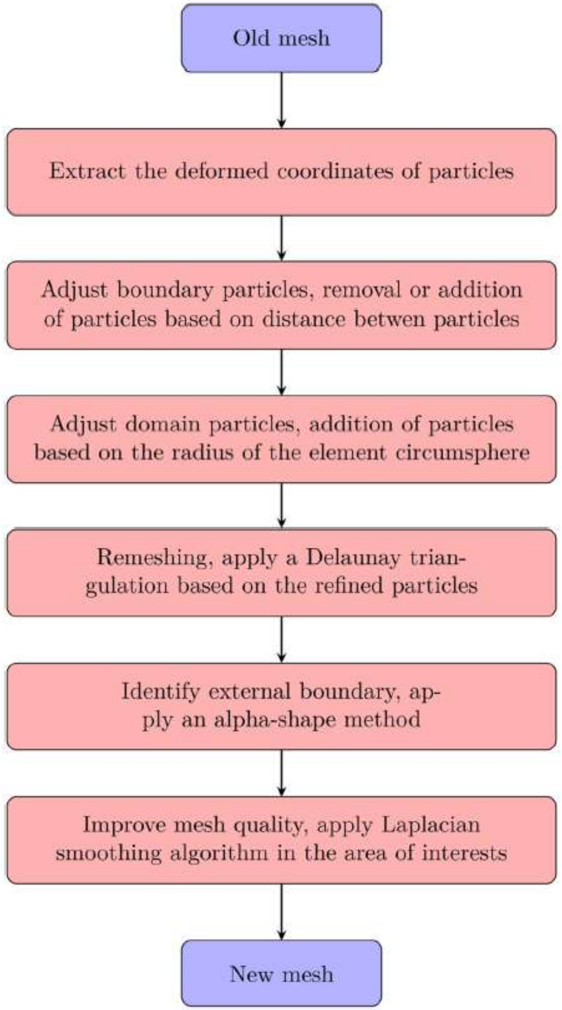

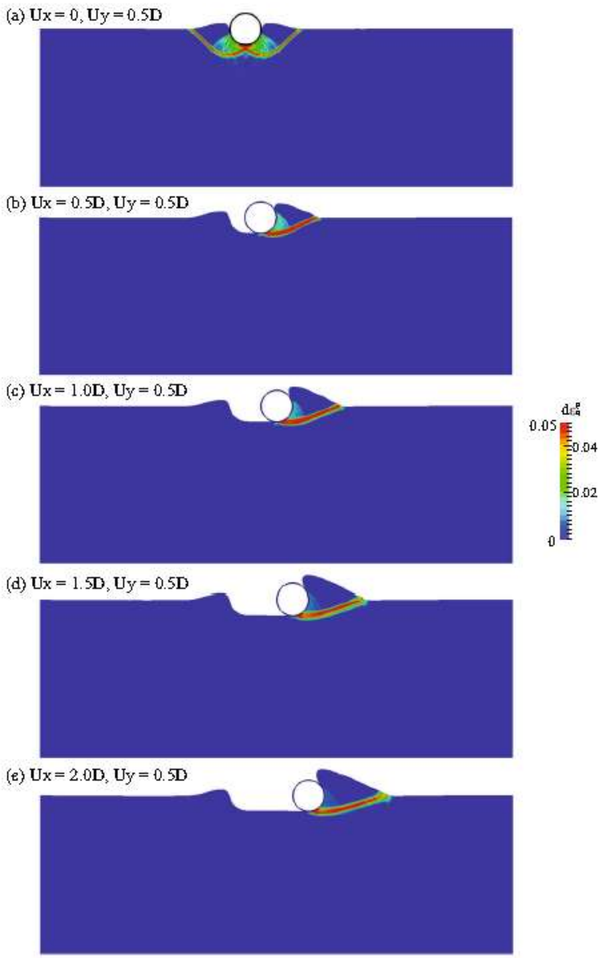

YUAN Wei-Hai, WANG Hao-Cheng, **ZHANG Wei**(*), et al. Particle Finite Element Method implementation for large deformation analysis using Abaqus. Acta Geotechnica, 2021, doi: 10.1007/s11440-020-01124-2

Comments on SPFEM

- E Oñate, 2020, CMAME：

However, only very recently the use of nodal integration in a PFEM framework has been investigated and successfully applied to geotechnical problems [12,13]. In these works, the authors proposed the so-called Smoothed Particle Finite Element Method (SPFEM), inspired by the well-established Smoothed Finite Element Method (SFEM) [14–17].

- E Oñate, 2020, ACME ,

A State of the Art Review of the Particle Finite Element Method (PFEM)

8.2 PFEM with Nodal Integration

Traditionally, the PFEM has been formulated for standard elemental integration, storing stresses and strains at the Gauss points. However, in PFEM with Gaussian integration, due to the continuous elimination of the elements done during the remeshing steps, it may be required to transfer the elemental information from the old mesh to the new one. This is avoided in fluid dynamics problems, where the measures of stresses and strains are computed from the scratch at each time step, but is mandatory for non-linear solid mechanics methods that require the storage of historical variables. Remapping procedures, besides having a certain computational cost, introduce interpolation errors into the numerical scheme and cause the smoothing of the historical variables (Sect. 2).

On the other hand, in nodal integration methods, stresses and material historical variables are computed and stored at the mesh nodes[99]. Consequently, a PFEM strategy with nodal integration does not require variable remapping procedures along the remeshing step.

This feature motivated recent research on the use of nodal integration in a PFEM framework[56, 124, 126]. The method, called by the authors Smoothed Particle Finite Element Method, took inspiration from the Smoothed Finite Element Method[135] and was successfully applied to 2D geomechanics problems with large deformations.

目　录

隐式光滑粒子有限元法(iSPFEM)

□ 悬臂梁大变形

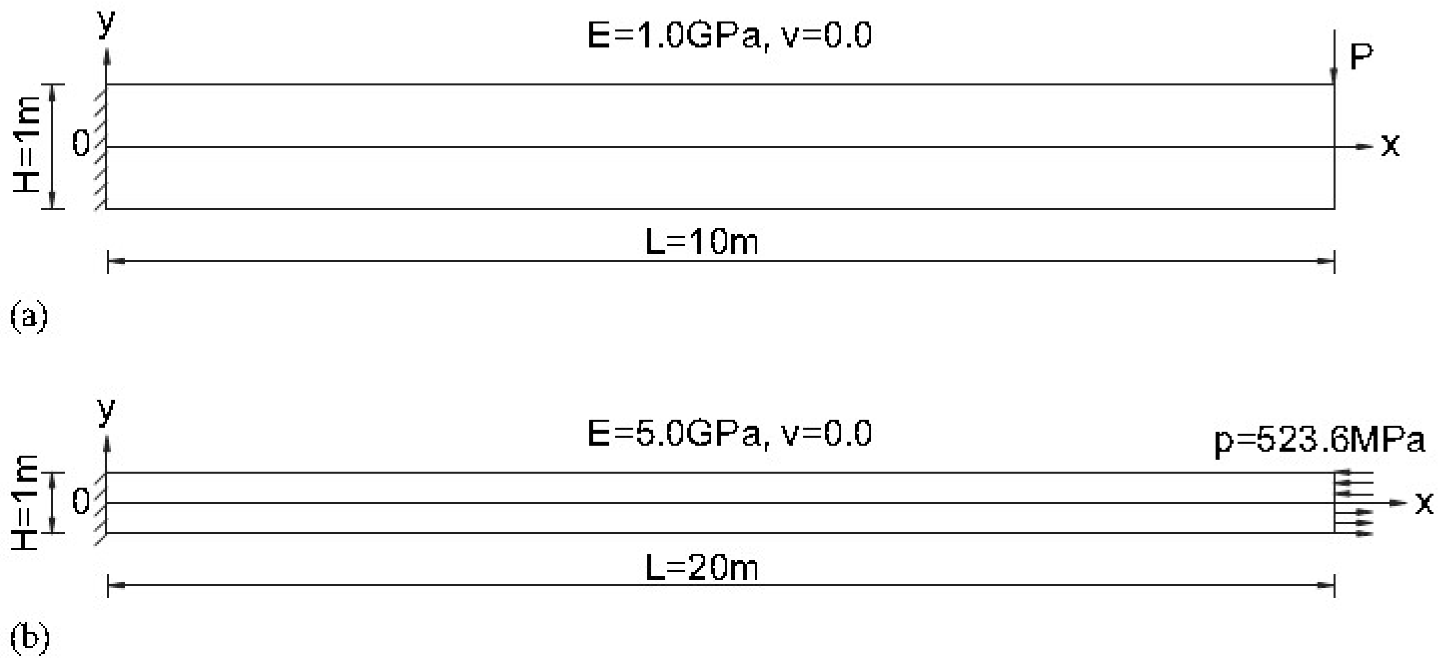

隐式光滑粒子有限元法(iSPFEM)

□ 悬臂梁大变形

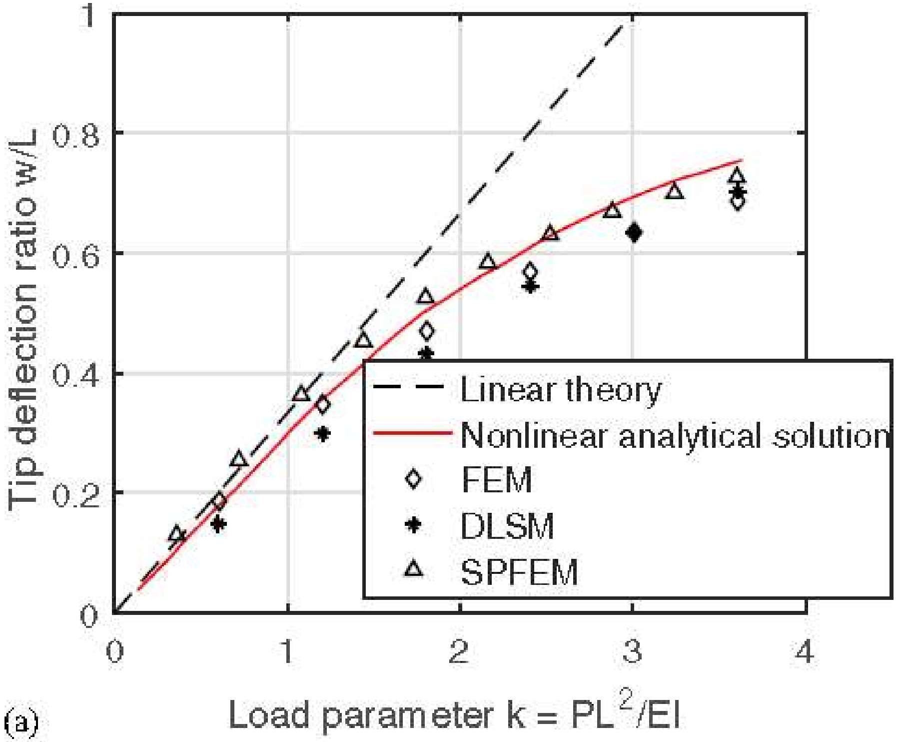

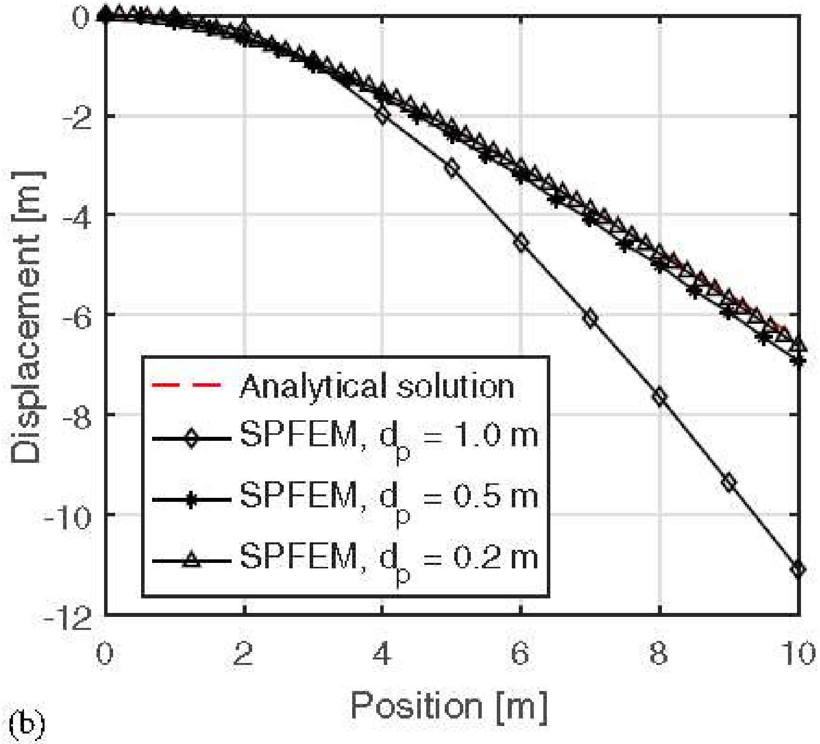

隐式光滑粒子有限元法(iSPFEM)

□ 悬臂梁大变形

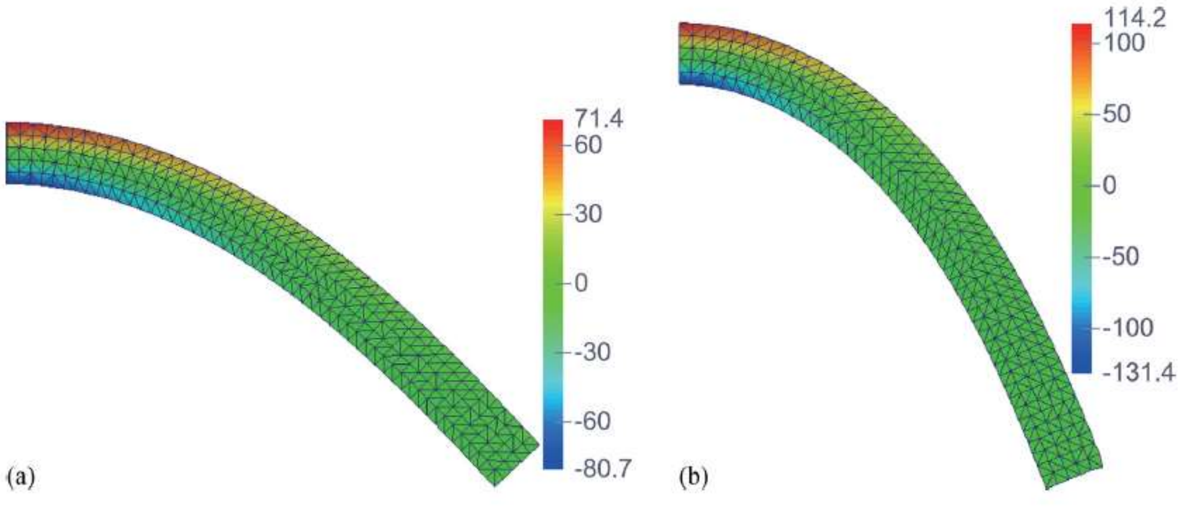

Fig. 5. Deformed configurations and the horizontal stress σ_{xx} distribution (unit: megapascals): (a) magnitude of concentrated load is 1,500 kPa; (b) magnitude of concentrated load is 3,000 kPa

隐式光滑粒子有限元法(iSPFEM)

□ 悬臂梁大变形

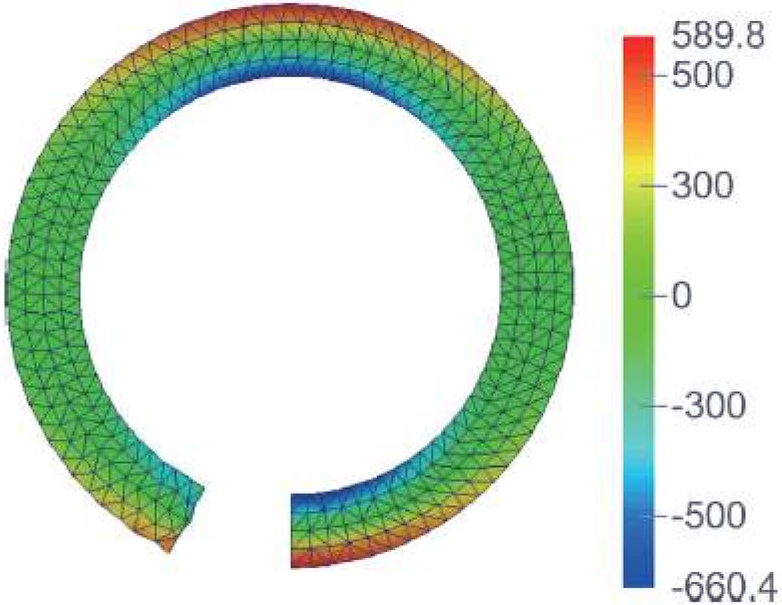

Fig. 6. Deformed configuration of the beam moment bending problem and the horizontal stress σ_{xx} distribution (unit: megapascals)

隐式光滑粒子有限元法(iSPFEM)

□ 土体旁压试验

Cavity expansion in Tresca soil

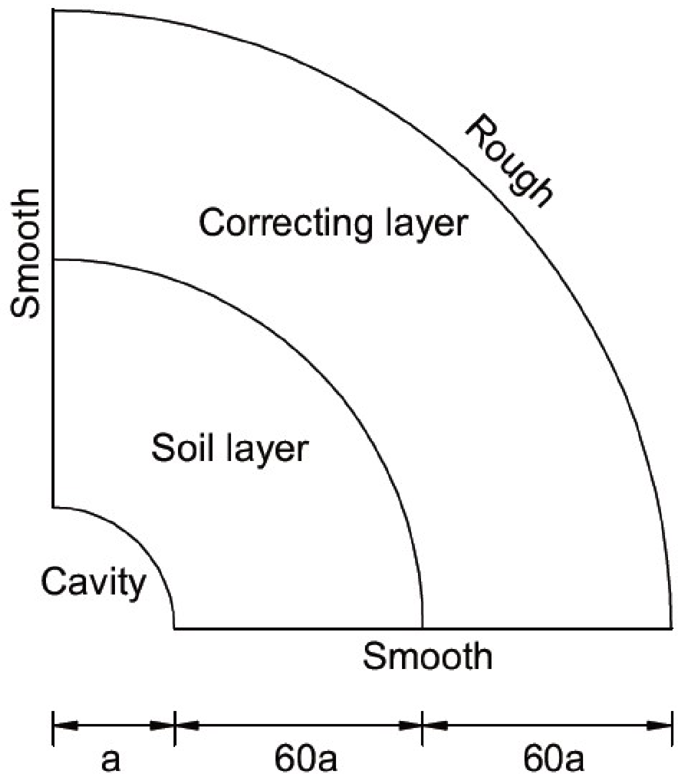

Soil:
E=461.5kPa
v=0.499
c_u=8.66kPa

Correcting layer:
E=166.67kPa
v=0.25

Details in:
Zhang, W., ***Yuan, W.-H.****, Dai, B.-B., 2017. A smoothed particle finite element method for large-deformation problems in geomechanics. International Journal of Geomechanics. DOI: 10.1061/(ASCE)GM.1943-5622.0001079.*

隐式光滑粒子有限元法(iSPFEM)

□ 土体旁压试验

Cavity expansion in Tresca soil

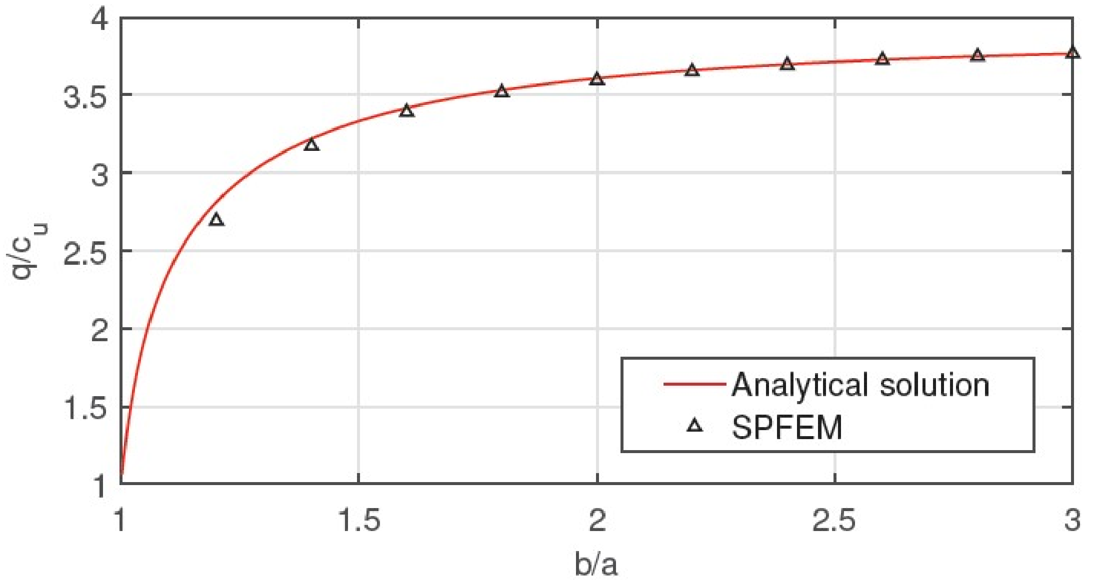

Figure: Normalized internal pressure q/c_u versus normalized radial displacement b/a.

隐式光滑粒子有限元法(iSPFEM)

口 土体旁压试验

Cavity expansion in Tresca soil

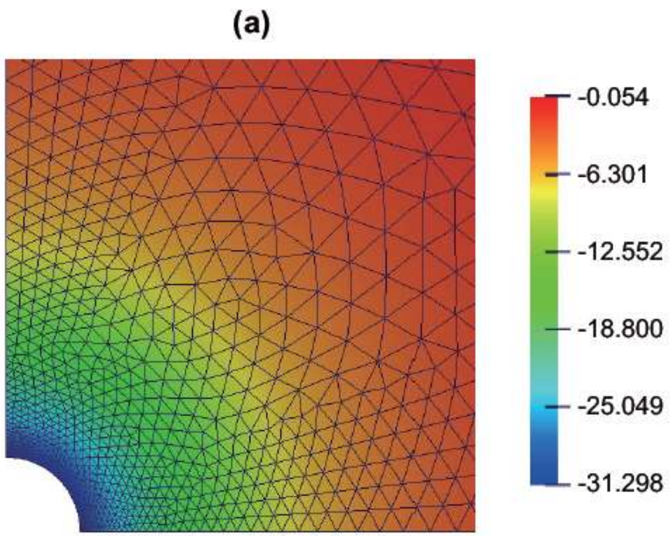

Figure: Deformed configuration of the cavity expansion problem and the radial stress σ_r distribution (unit: kPa): (a) Normalized radial displacement $b/a = 2$; (b) Normalized radial displacement $b/a = 3$

□ 软土地基上的条形基础

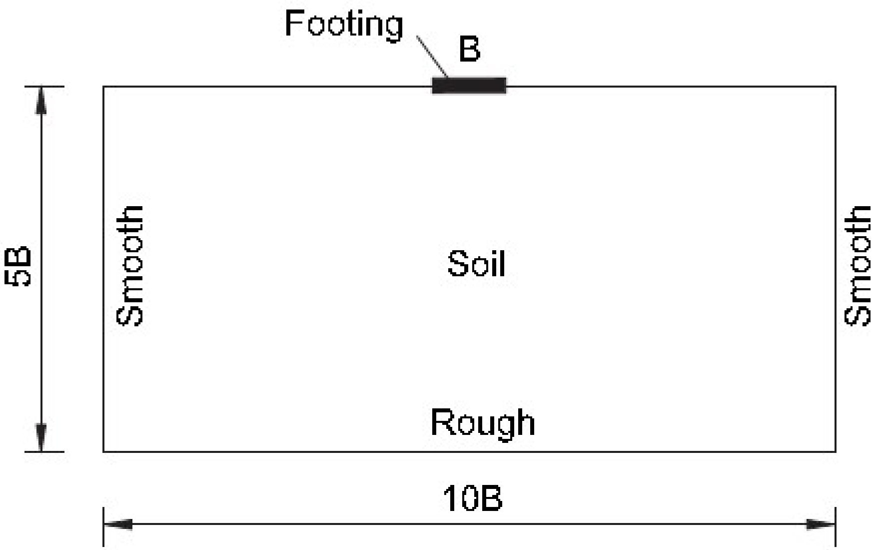

Soil：

E=100kPa

v=0.495

c_u=1kPa

隐式光滑粒子有限元法(iSPFEM)

❑ 软土地基上的条形基础

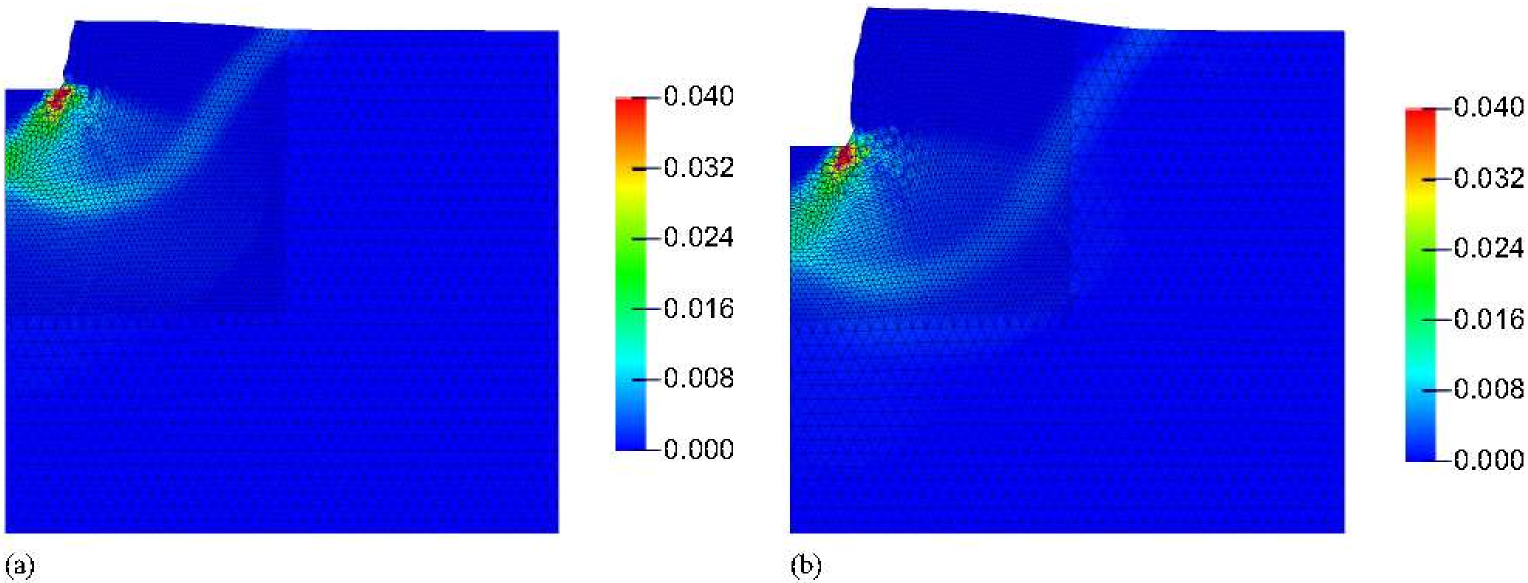

Fig. 11. Mesh of the footing problem and the incremental deviatoric plastic strain invariant distribution: (a) normalized penetration, $z/B = 0.5$; (b) normalized penetration, $z/B = 1.0$

隐式光滑粒子有限元法(iSPFEM)

ロ 软土地基上的条形基础

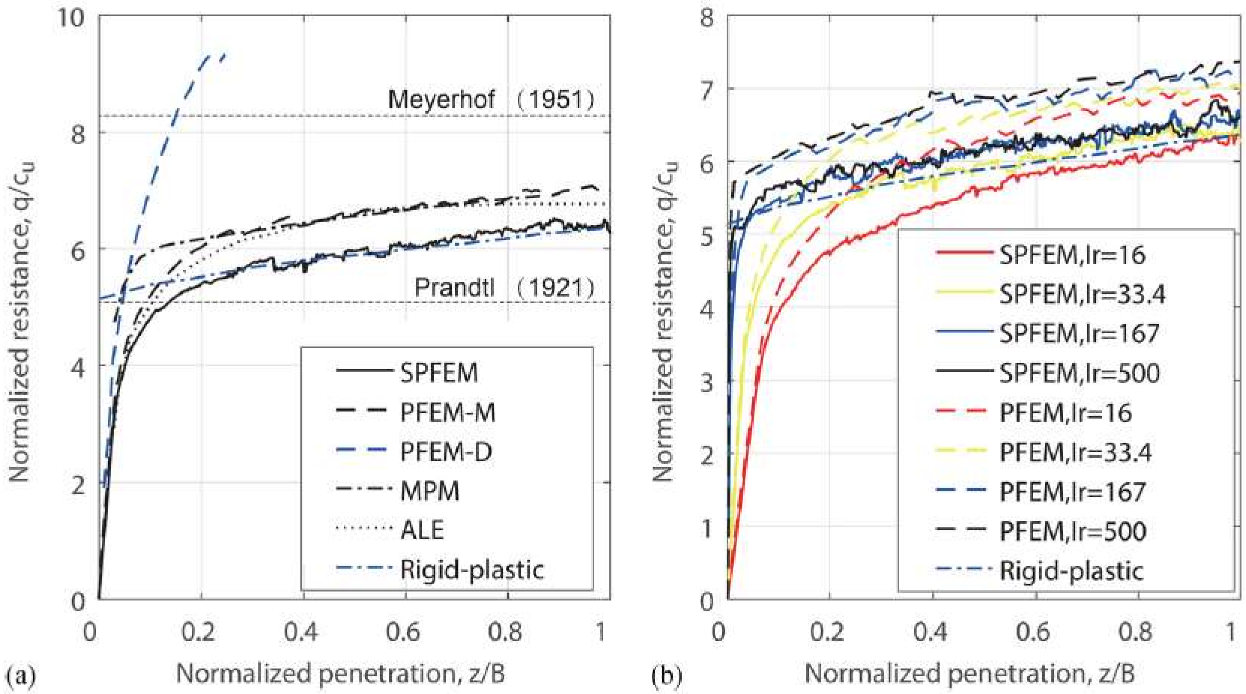

Fig. 12. Normalized load-displacement curves for rigid footing on Tresca soil: (a) comparison with other numerical methods (I_r = 33.4); (b) comparison with PFEM at different I_r values

隐式光滑粒子有限元法(iSPFEM)

□ 边坡大变形失稳

Failure of a homogeneous soil slope

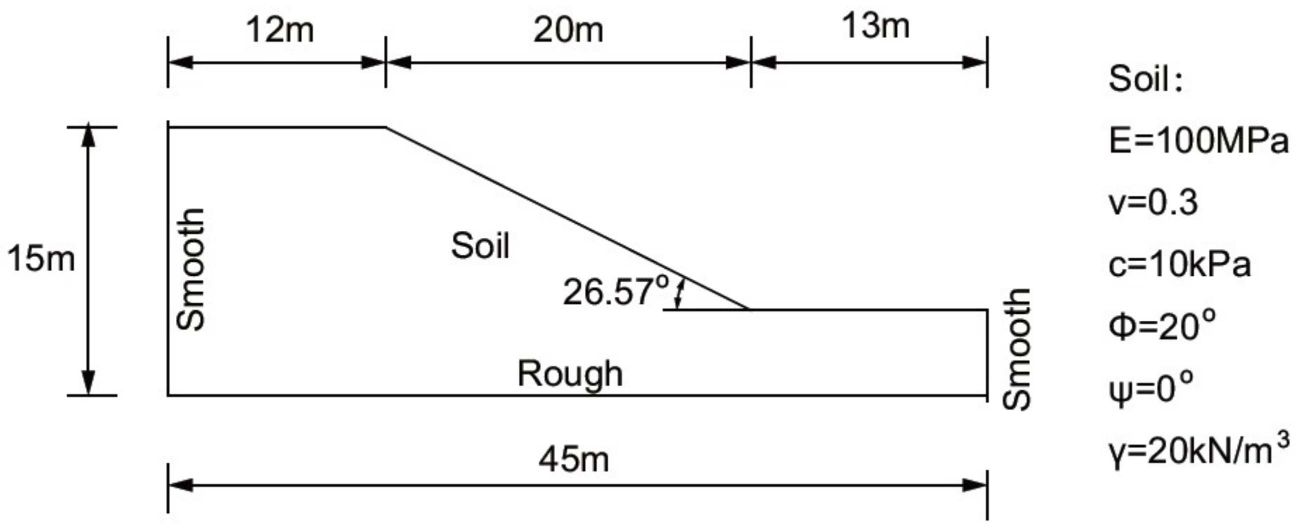

Figure: Failure of a homogeneous soil slope

Details in:
Zhang, W., ***Yuan, W.-H.****, Dai, B.-B., 2017. A smoothed particle finite element method for large-deformation problems in geomechanics. International Journal of Geomechanics. DOI: 10.1061/(ASCE)GM.1943-5622.0001079.*

隐式光滑粒子有限元法(iSPFEM)

□ 边坡大变形失稳

Failure of a homogeneous soil slope

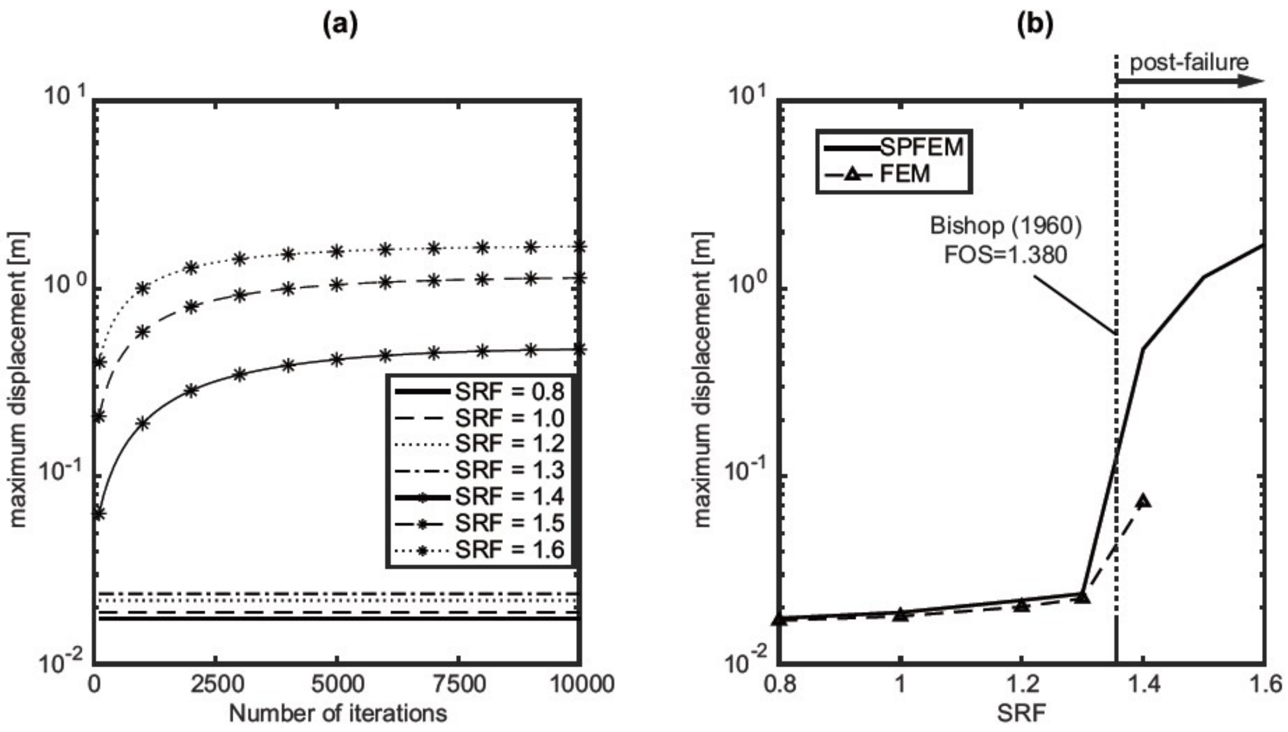

Figure: (a) Maximum displacement versus number of iterations; (b) Maximum displacement with different values of SRF.

隐式光滑粒子有限元法(iSPFEM)

□ 边坡大变形失稳

Failure of a homogeneous soil slope

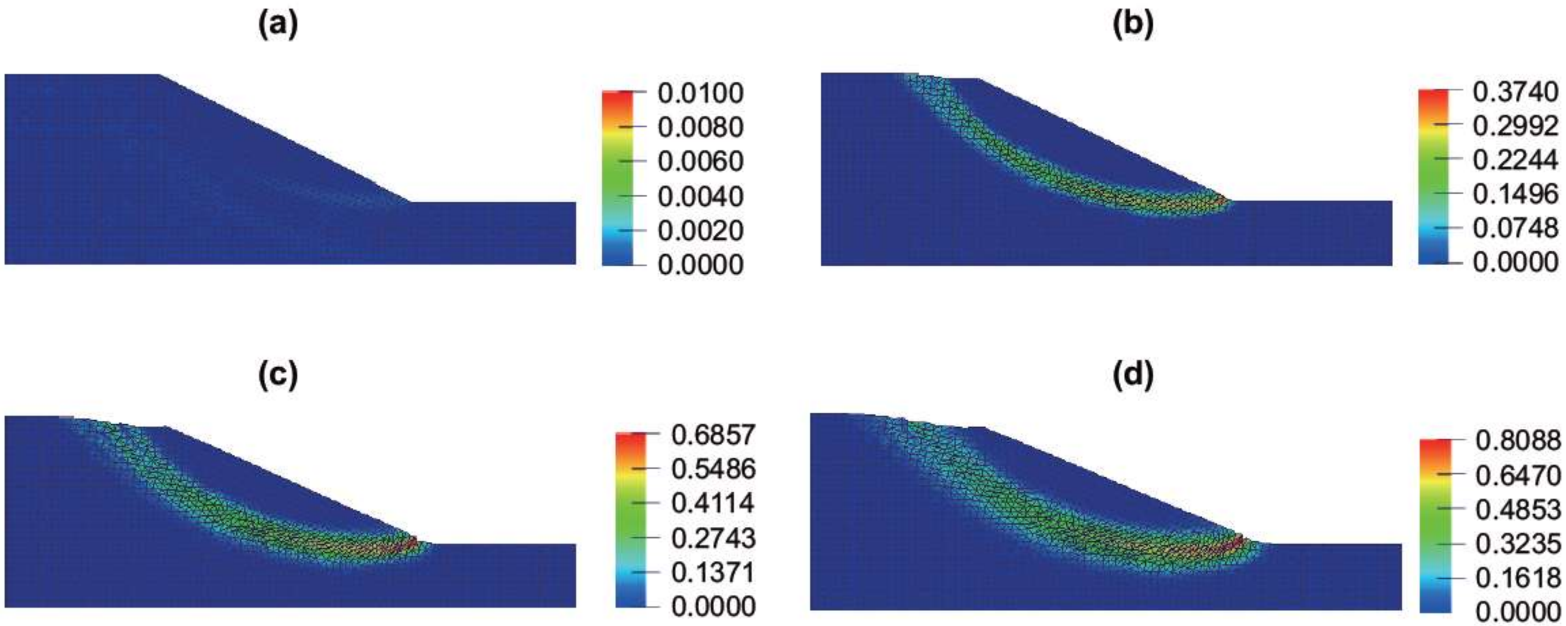

Figure: Configurations of the slope problem and the incremental deviatoric plastic strain invariant distribution: (a) $SRF = 1.3$; (b) $SRF = 1.4$; (c) $SRF = 1.5$; (d) $SRF = 1.6$

显式光滑粒子有限元法(eSPFEM)

□ 一维杆振动

Axial vibration of a continuum bar

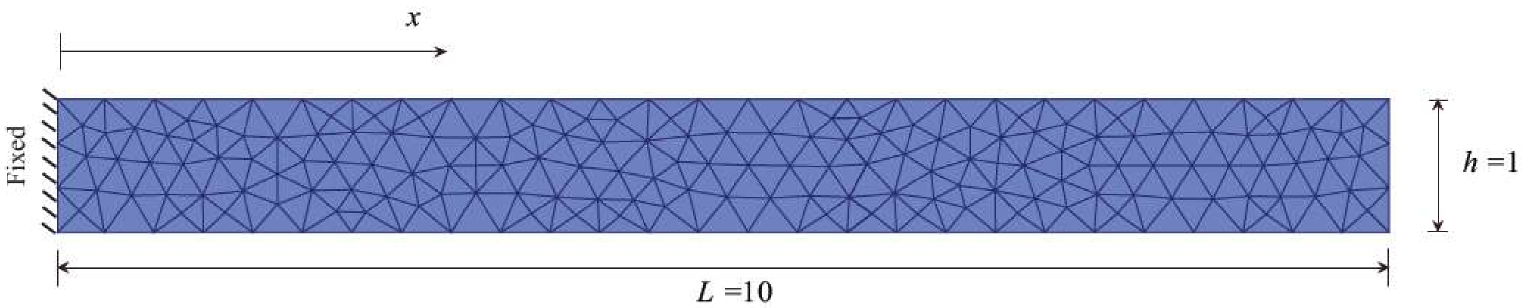

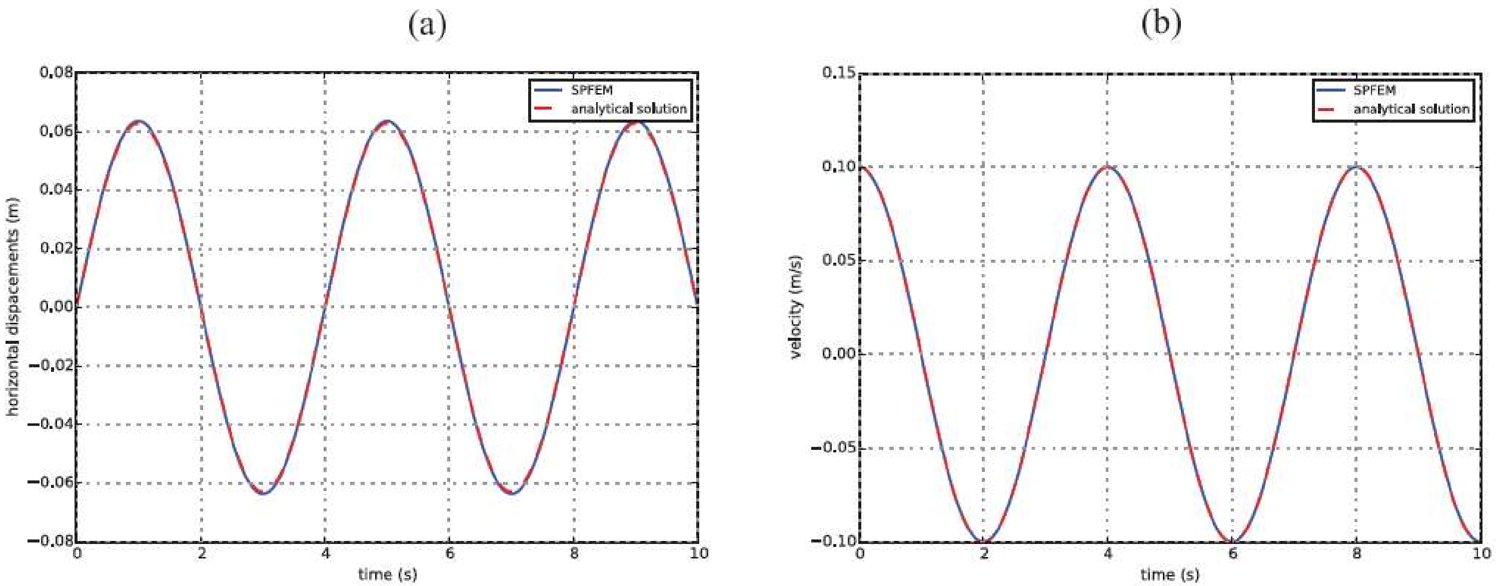

显式光滑粒子有限元法(eSPFEM)

□ 软土地基上的条形基础

Rigid footing on Tresca soil

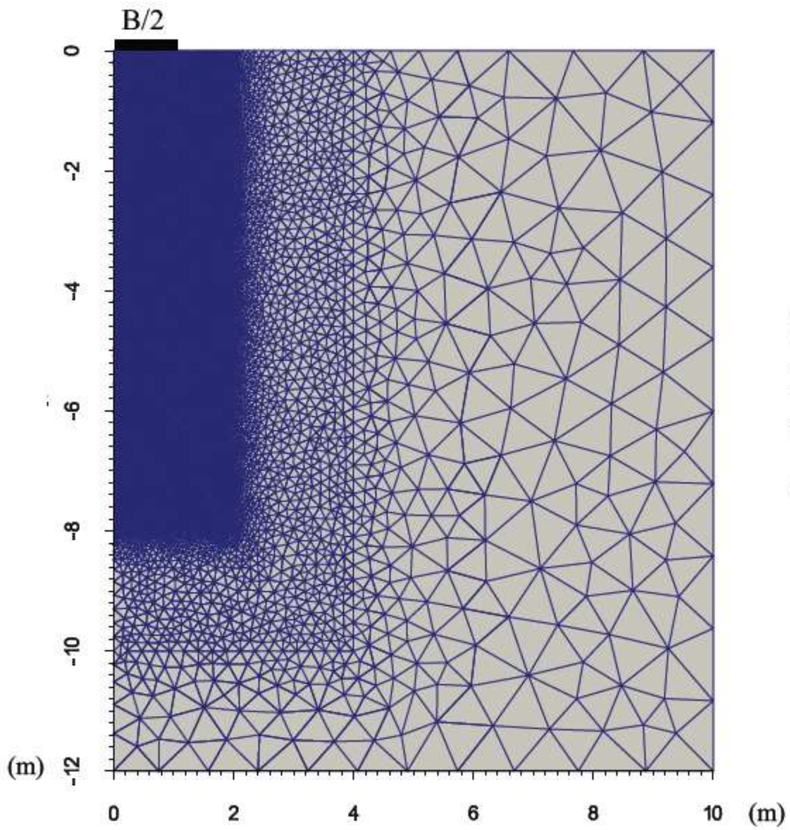

Soil:
E=100kPa
ν=0.495
c_u=1kPa

Figure: Geometry and mesh of the footing problem.

显式光滑粒子有限元法(eSPFEM)

□ 软土地基上的条形基础

Rigid footing on Tresca soil

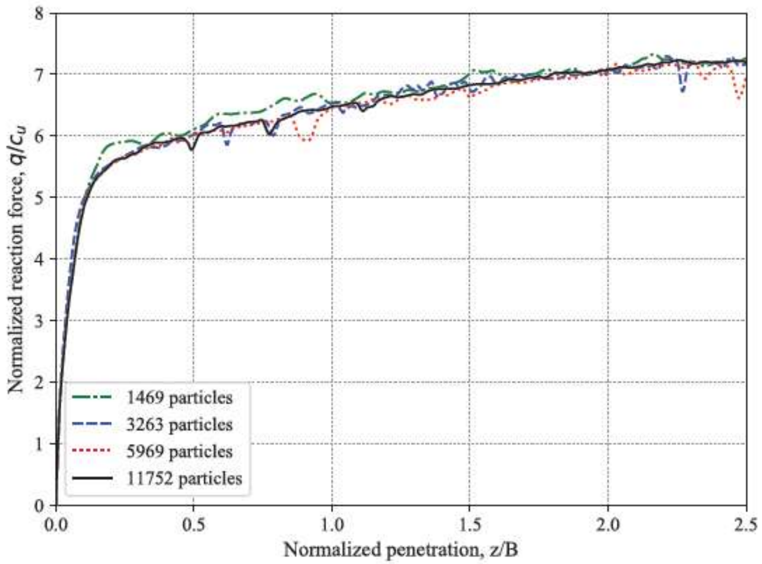

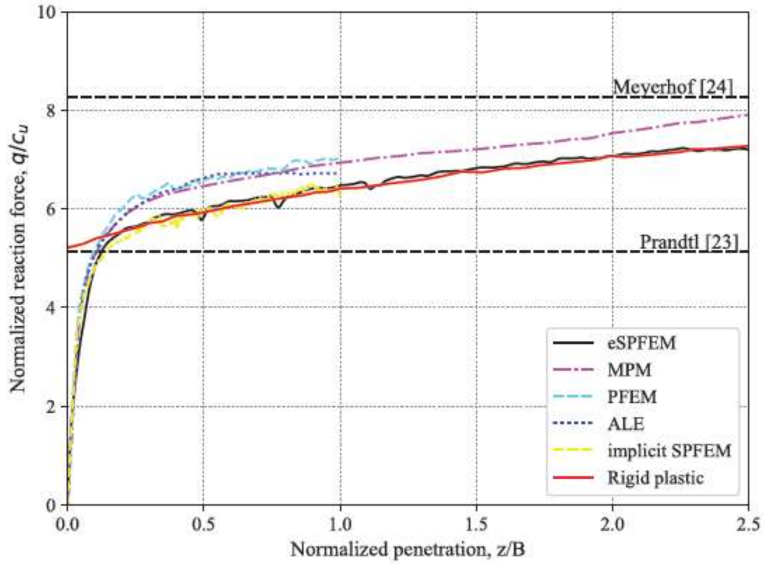

Figure: Normalized load-displacement curves for rigid footing on Tresca soil: (a) Different particle densities; (b) Comparison with other numerical methods

显式光滑粒子有限元法(eSPFEM)

□ **软土地基上的条形基础**

Rigid footing on Tresca soil

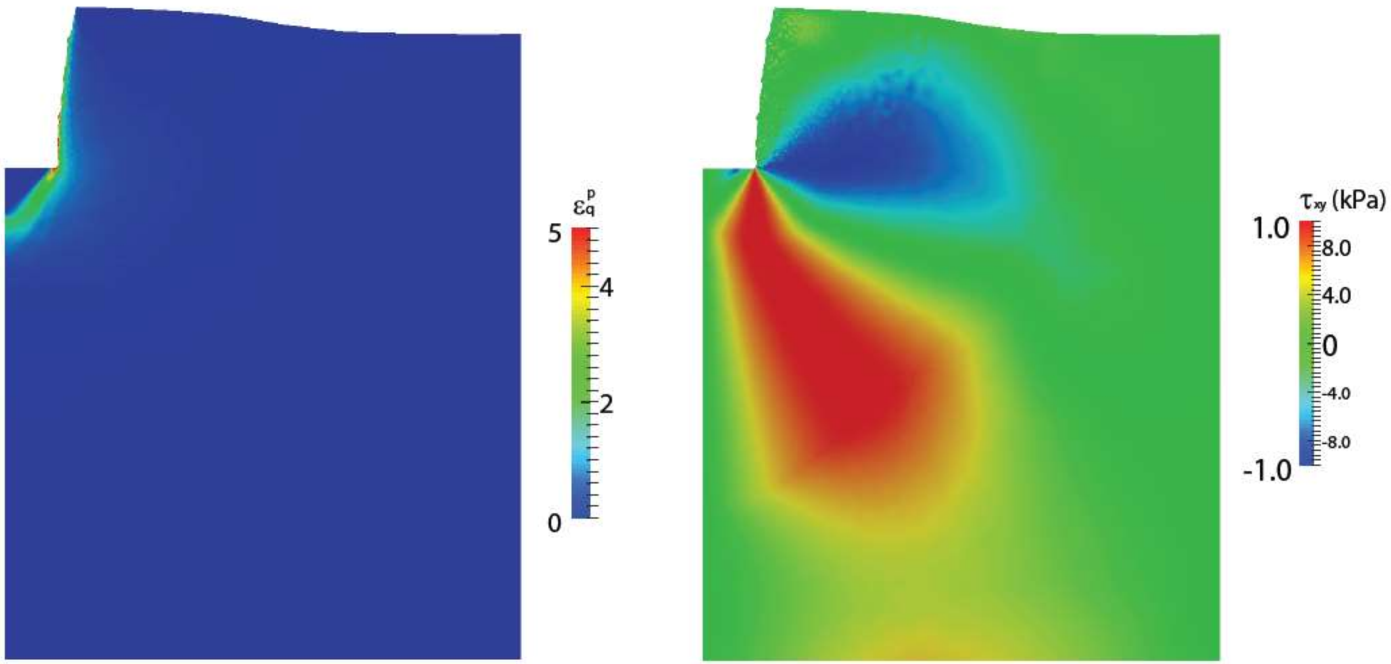

Figure: Contour of accumulated plastic strains (a) and shear stress (b) at a penetration depth of 2.5 m

显式光滑粒子有限元法(eSPFEM)

□ 砂柱垮塌

The collapse of two-dimensional sand columns

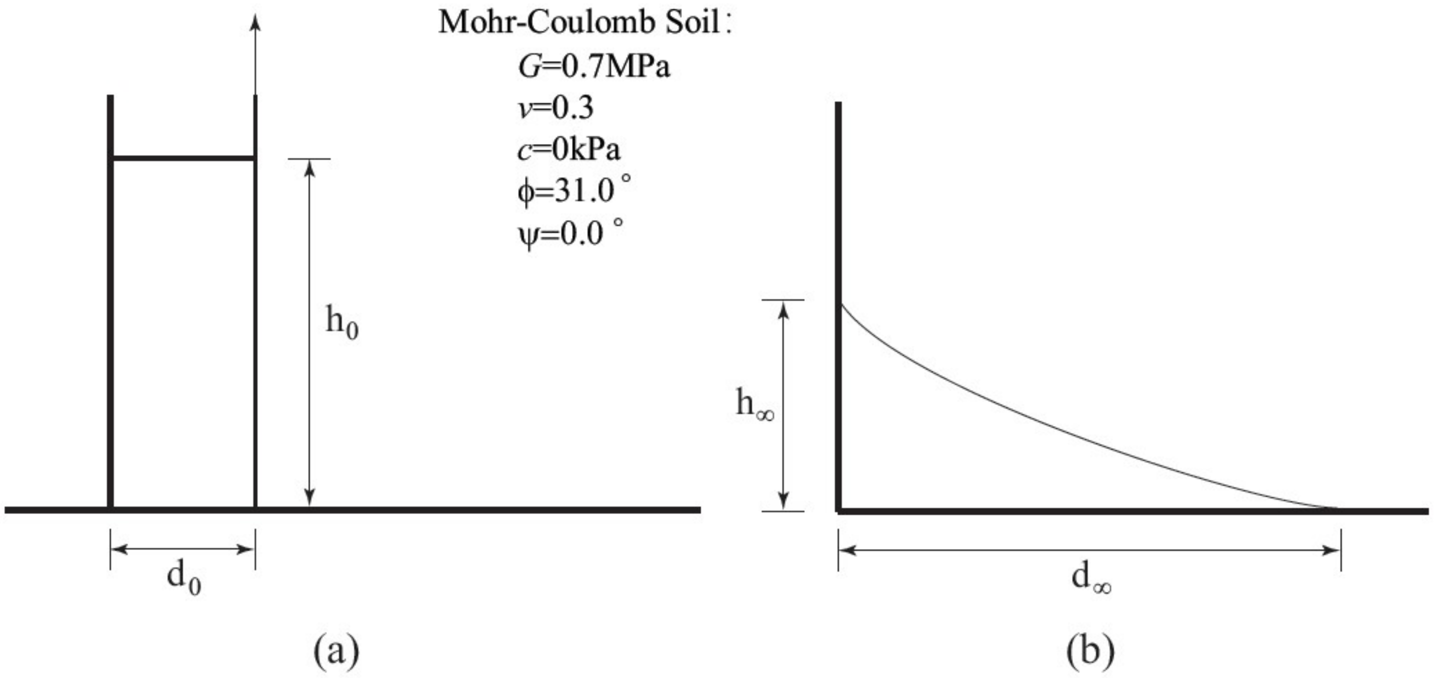

Figure: Initial setup (a) and final deposit (b) of Lube's experiments.

显式光滑粒子有限元法(eSPFEM)

□ 砂柱垮塌

The collapse of two-dimensional sand columns

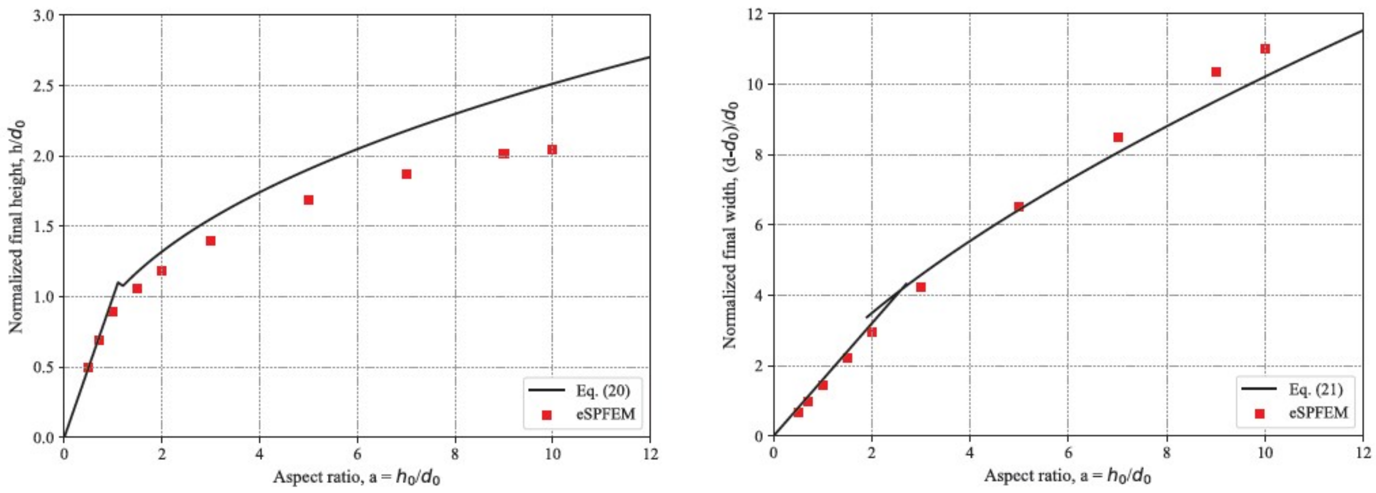

Figure: Normalized final height and width of granular columns as function of aspect ratio.

显式光滑粒子有限元法(eSPFEM)

□ 砂柱垮塌

The collapse of two-dimensional sand columns

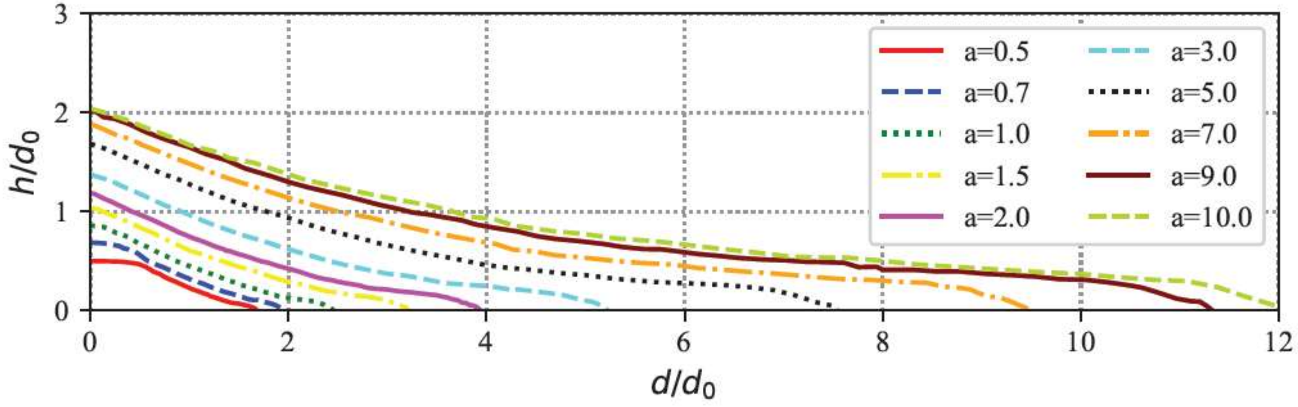

Figure: Final deposit profiles normalized to initial width for various aspect ratios.

显式光滑粒子有限元法(eSPFEM)

□ 铝棒垮塌

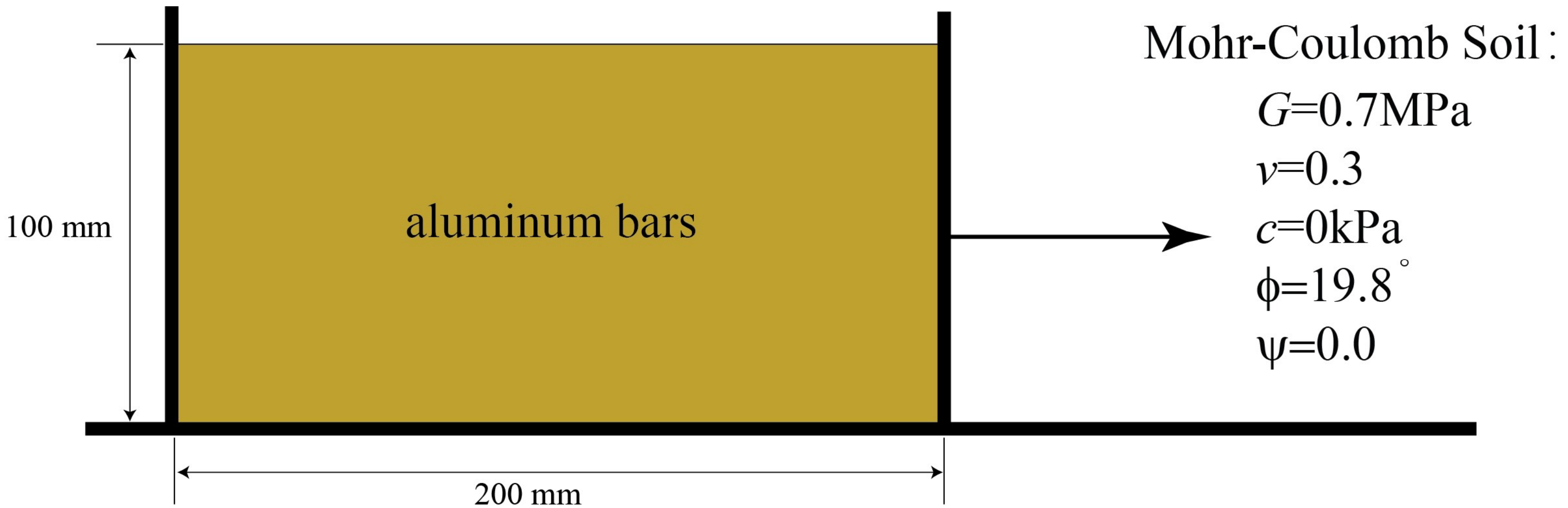

显式光滑粒子有限元法(eSPFEM)

□ 铝棒垮塌

显式光滑粒子有限元法(eSPFEM)

□ 铝棒垮塌

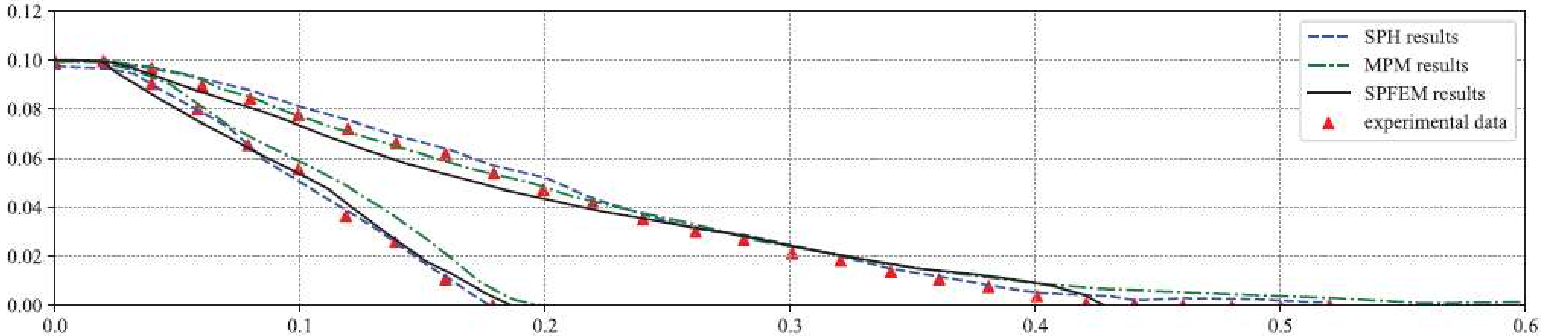

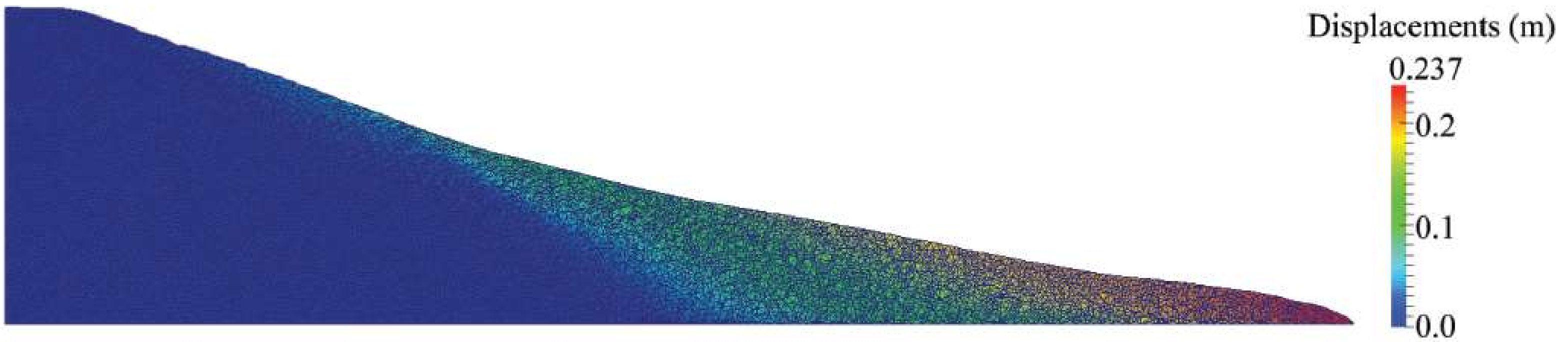

□ 长边坡渐进破坏

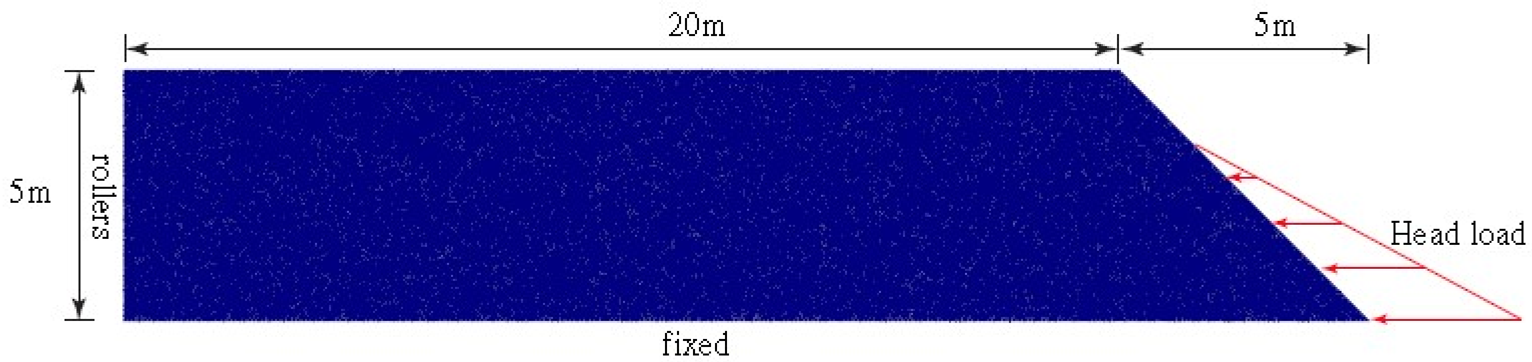

Fig. 15 Geometry and mesh for the strain-softening slope stability problem

显式光滑粒子有限元法(eSPFEM)

☐ 长边坡渐进破坏

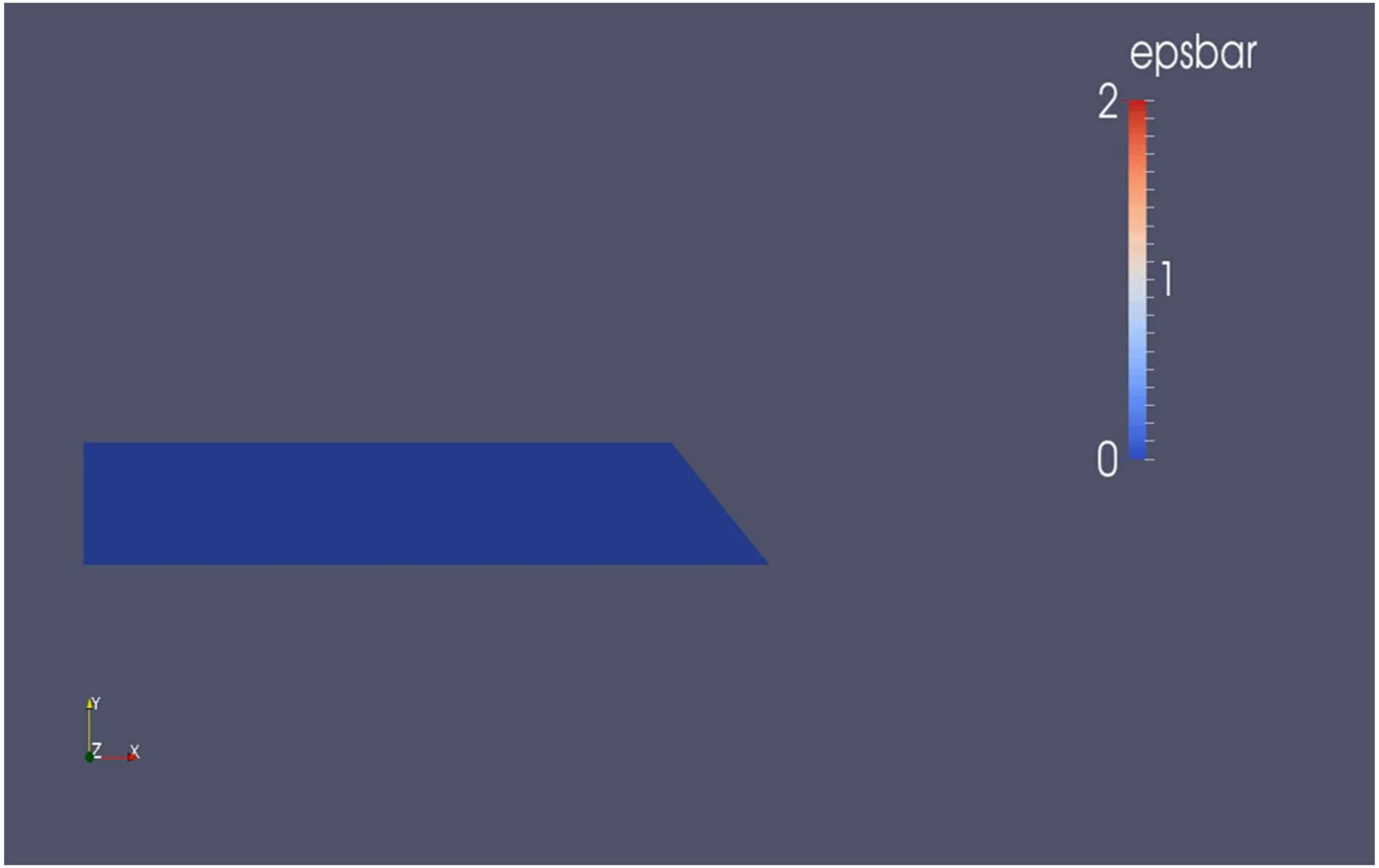

显式光滑粒子有限元法(eSPFEM)

☐ 长边坡渐进破坏

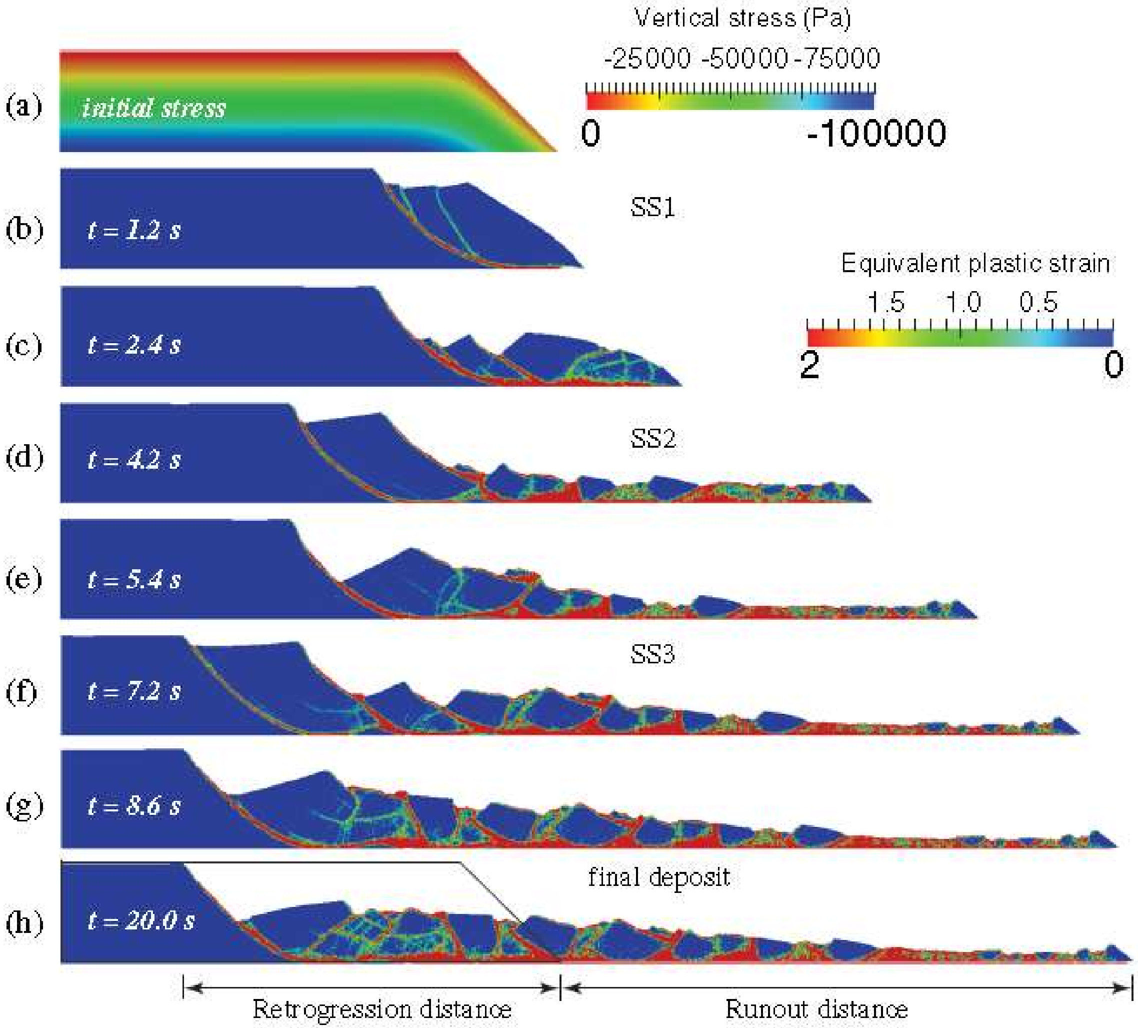

GPU并行三维显式光滑粒子有限元法

- 铝棒垮塌

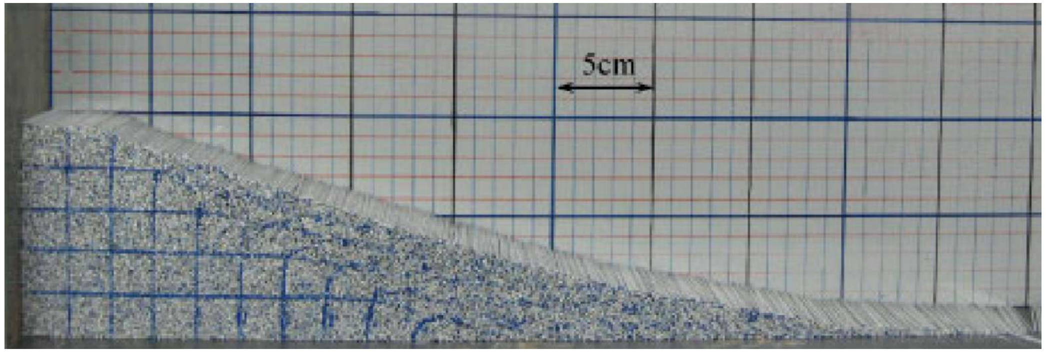

(Bui, 2008)

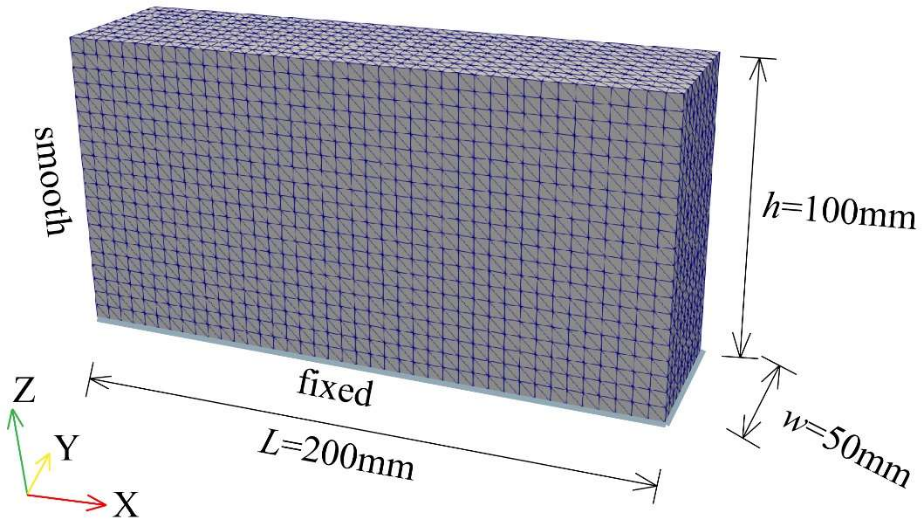

Shear modulus: 0.7MPa

Poisson's ratio: 0.3

Density: 2650kg/m^3

Cohesion: 0kPa

Friction angle: 19.8^o

Mohr-Coulomb model is used

GPU并行三维显式光滑粒子有限元法

□ 铝棒垮塌

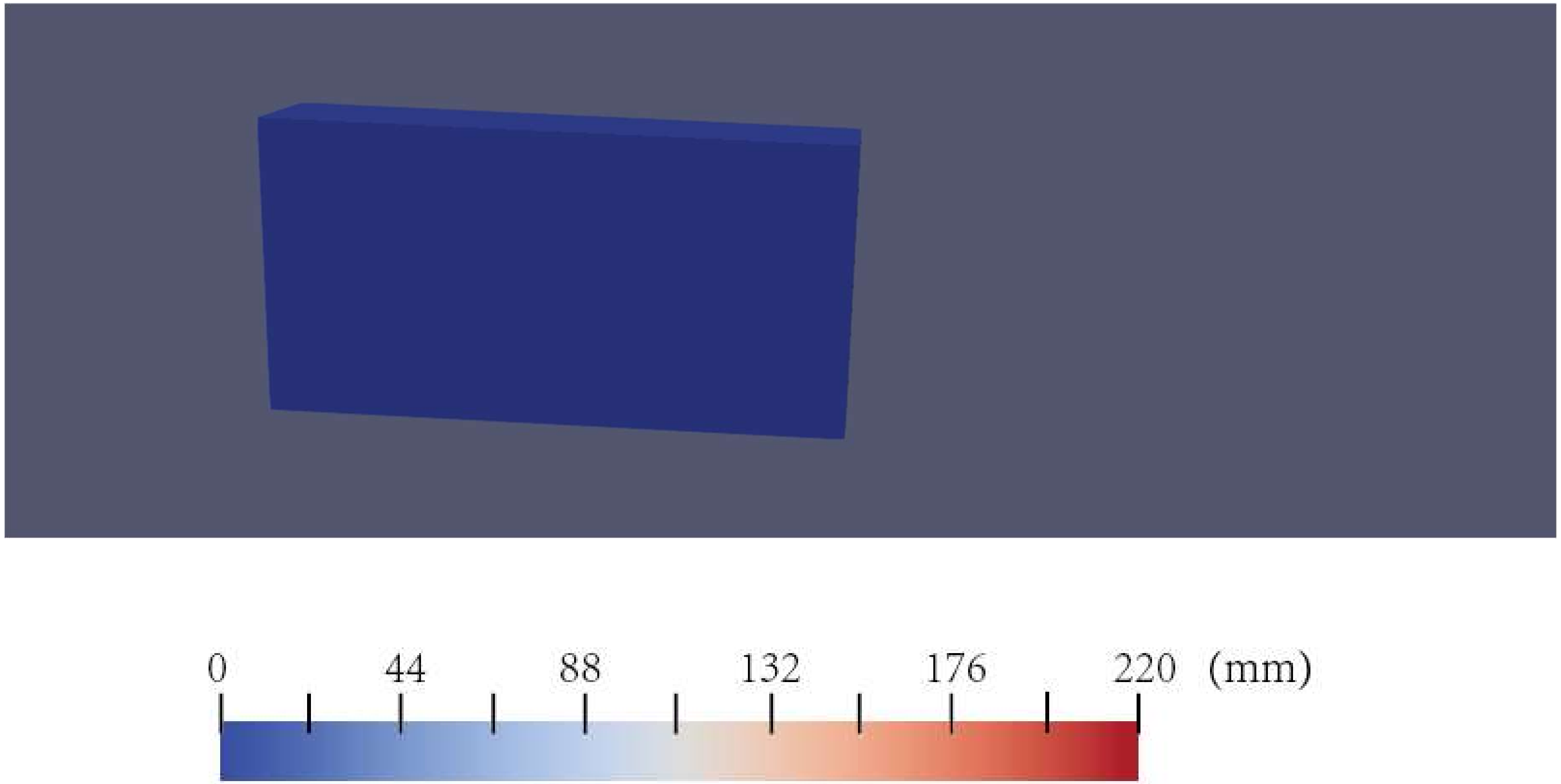

GPU并行三维显式光滑粒子有限元法

- 铝棒垮塌

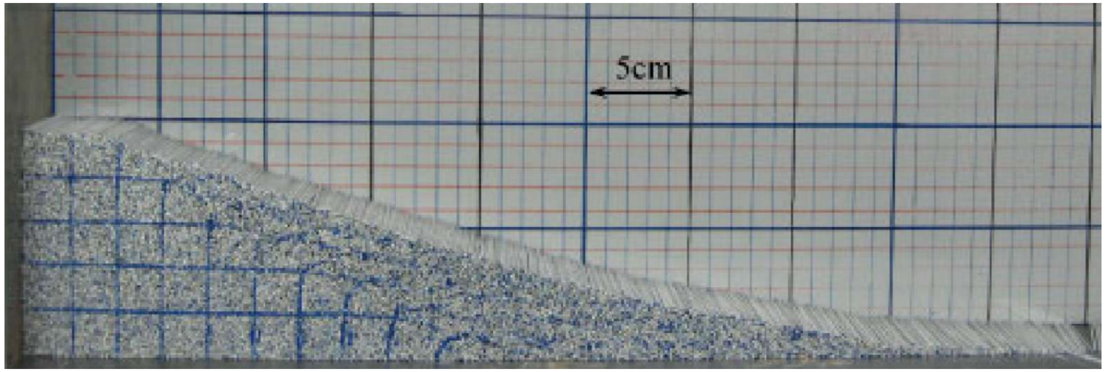

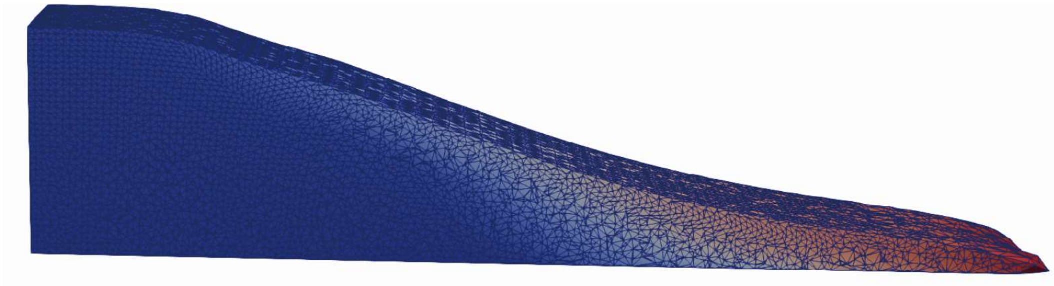

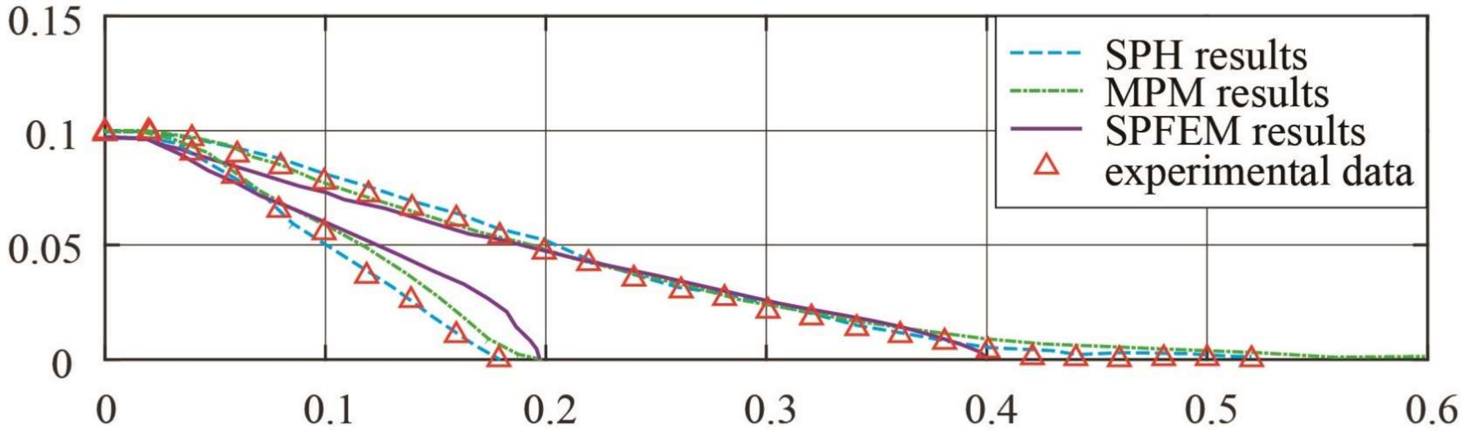

GPU并行三维显式光滑粒子有限元法

□ 铝棒垮塌

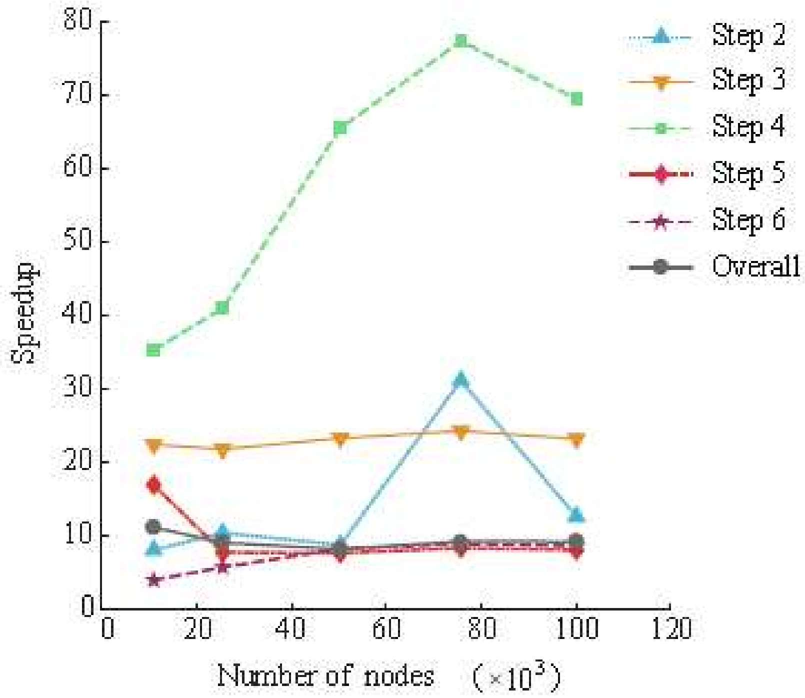

Fig. 14. Speedup of the double-precision GPU simulations over sequential CPU simulations.

GPU并行三维显式光滑粒子有限元法

□ 长边坡渐进破坏

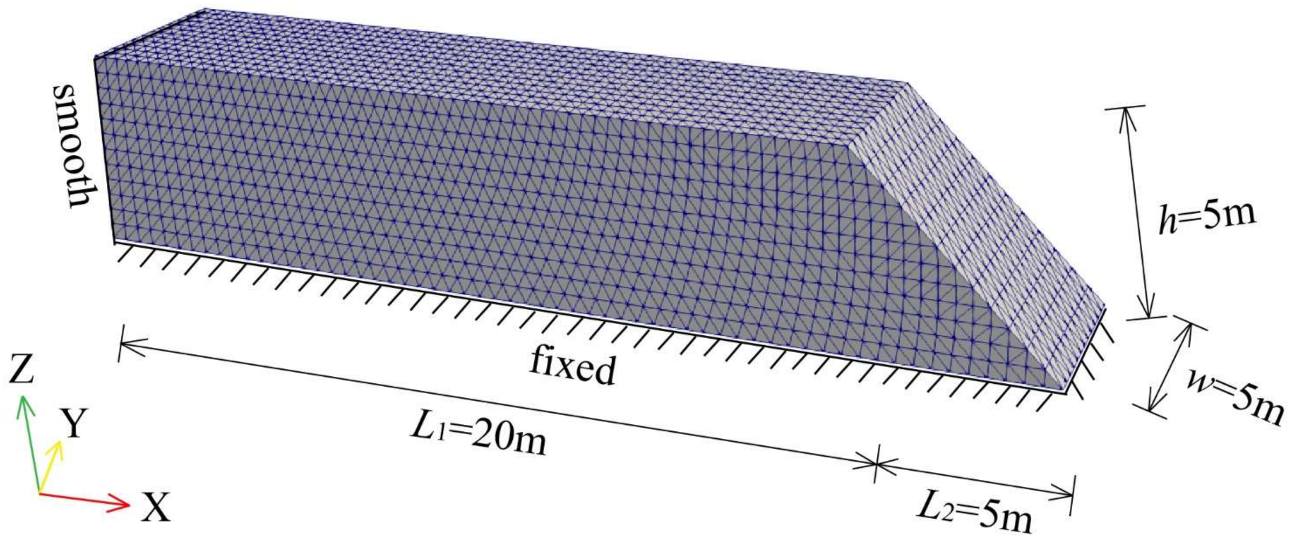

Young’s modulus: 1.0MPa

Poisson’s ratio: 0.33

Density: 2000kg/m^3

Cohesion(p): 20kPa

Cohesion(r): 4kPa

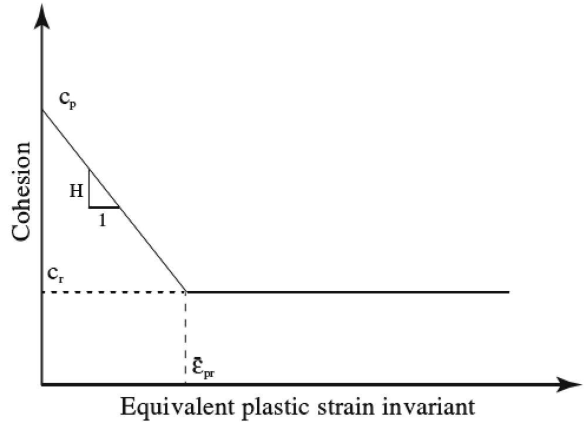

Concept of the cohesion softening model

GPU并行三维显式光滑粒子有限元法

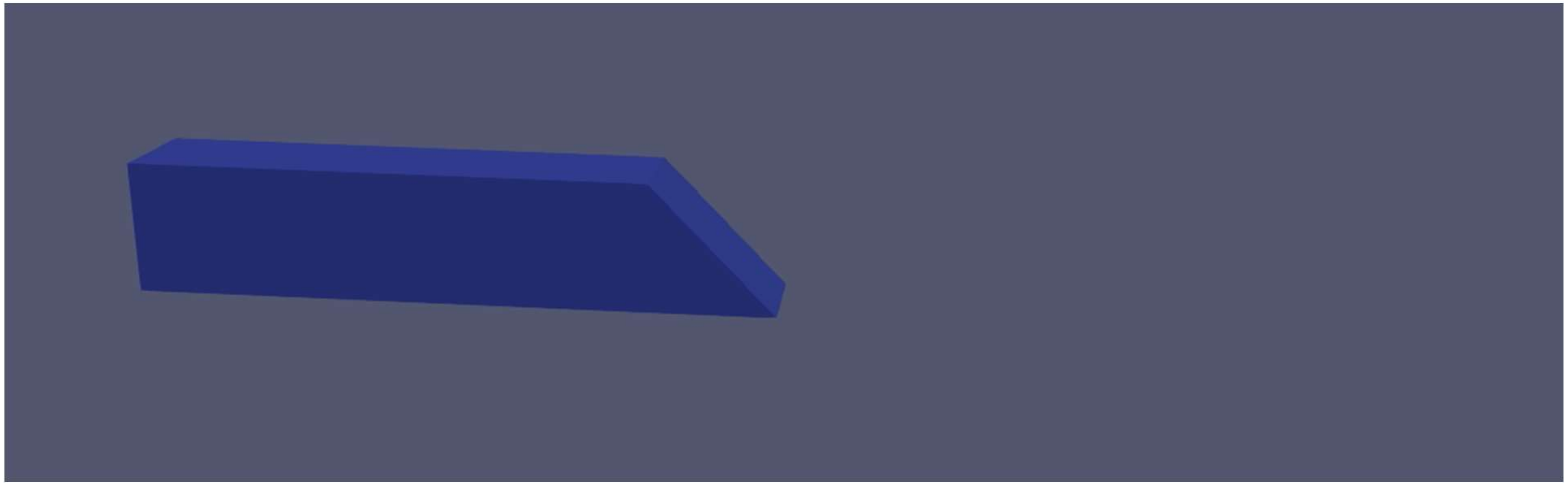

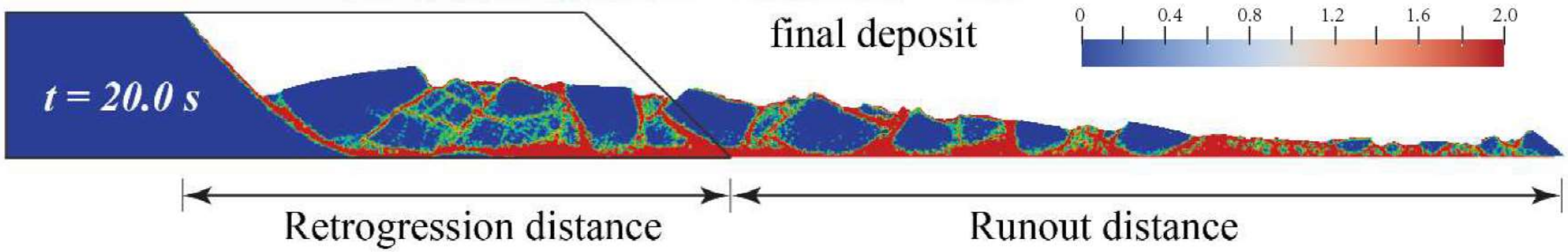

- ✓ With GPU acceleration, computation was completed in ~5 hours with ~250k nodes.
- ✓ Without GPU acceleration, computation was completed in ~13 hours with only ~ 38k nodes. (Zhang X, 2017)

□ 修正剑桥土(MCC)中的静力触探试验(CPT)

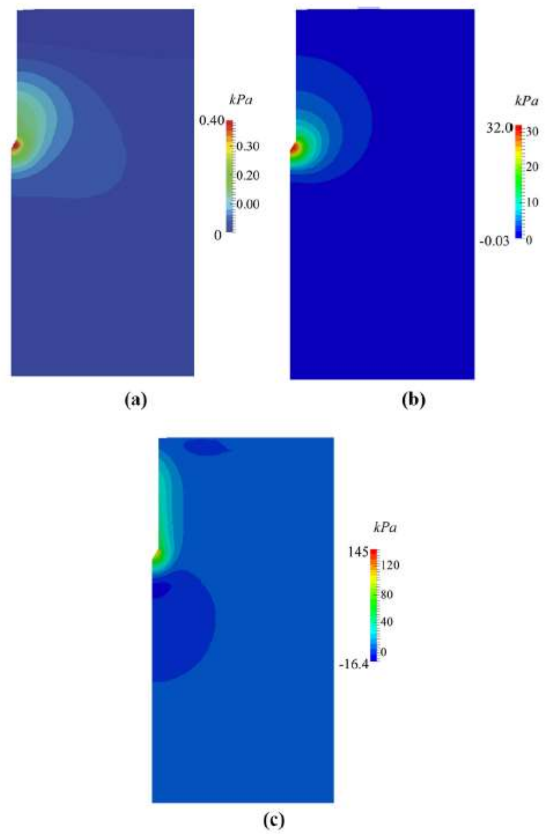

Notes: (a) excess pore water pressure, $k = 10^{-3} m/s$; (b) excess pore water pressure, $k = 10^{-5} m/s$; (c) excess pore water pressure, $k = 10^{-7} m/s$

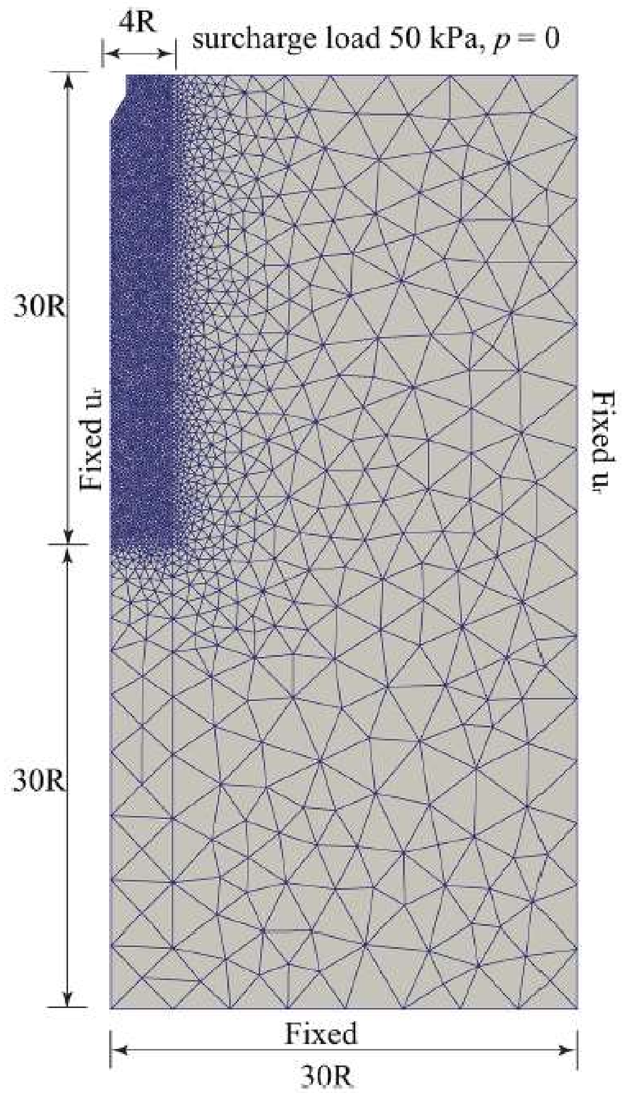

Abaqus粒子有限元法

□ 管线-土相互作用

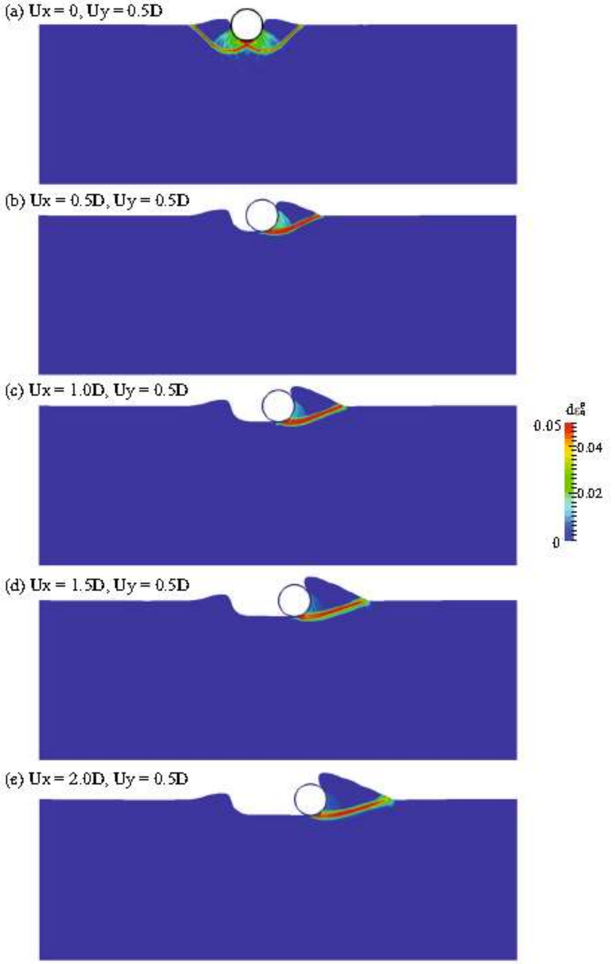

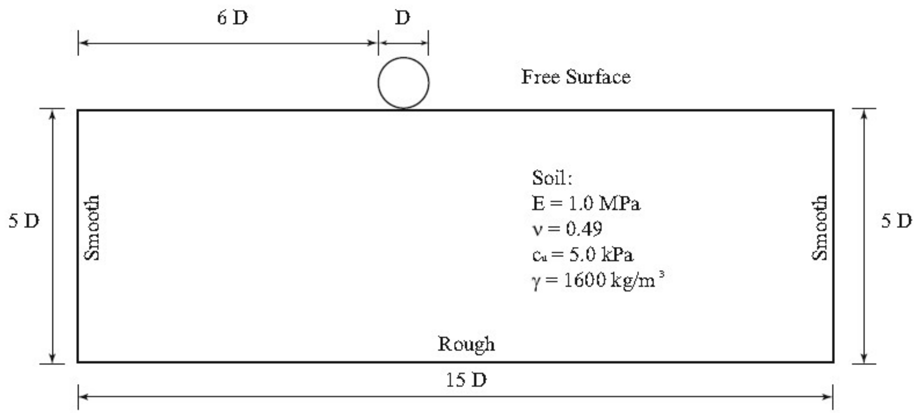

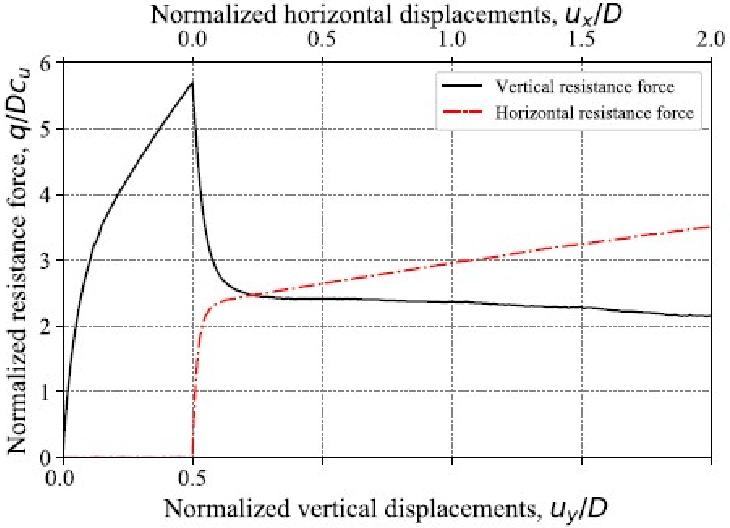

Fig. 19 Normalized resistance force versus displacements

基于SPFEM的CPT解析

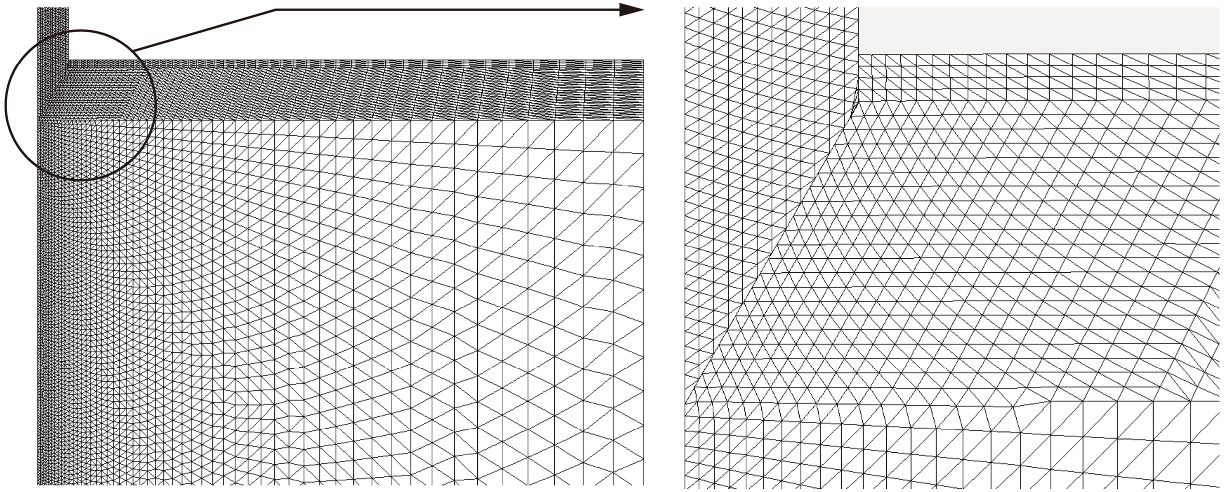

Initial Computation Mesh

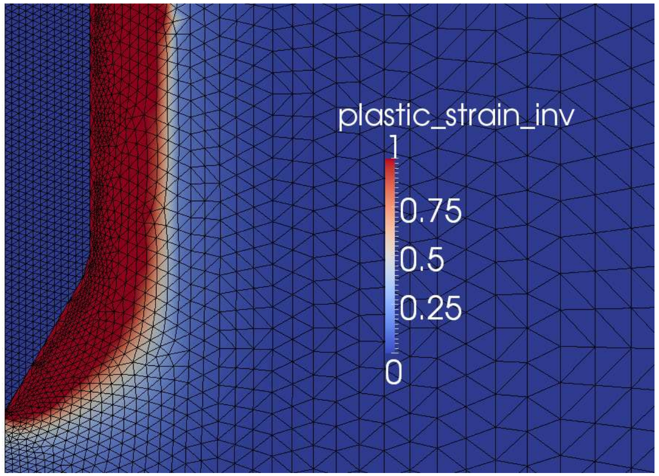

Final Computation Mesh

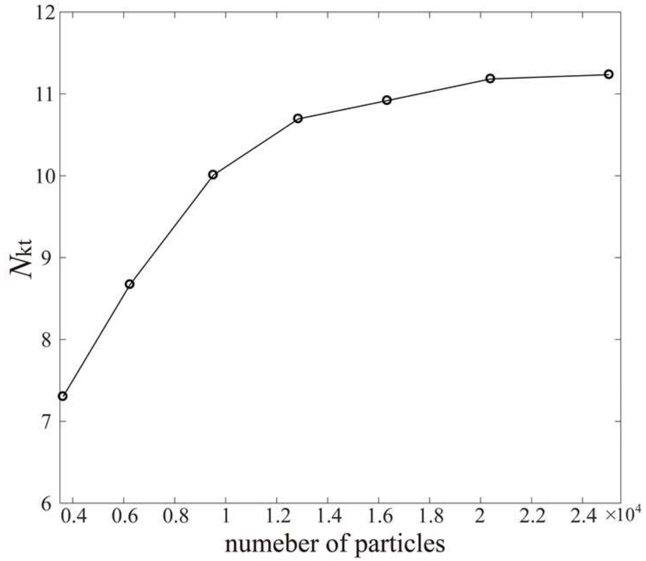

Effect of mesh density

基于SPFEM的CPT解析

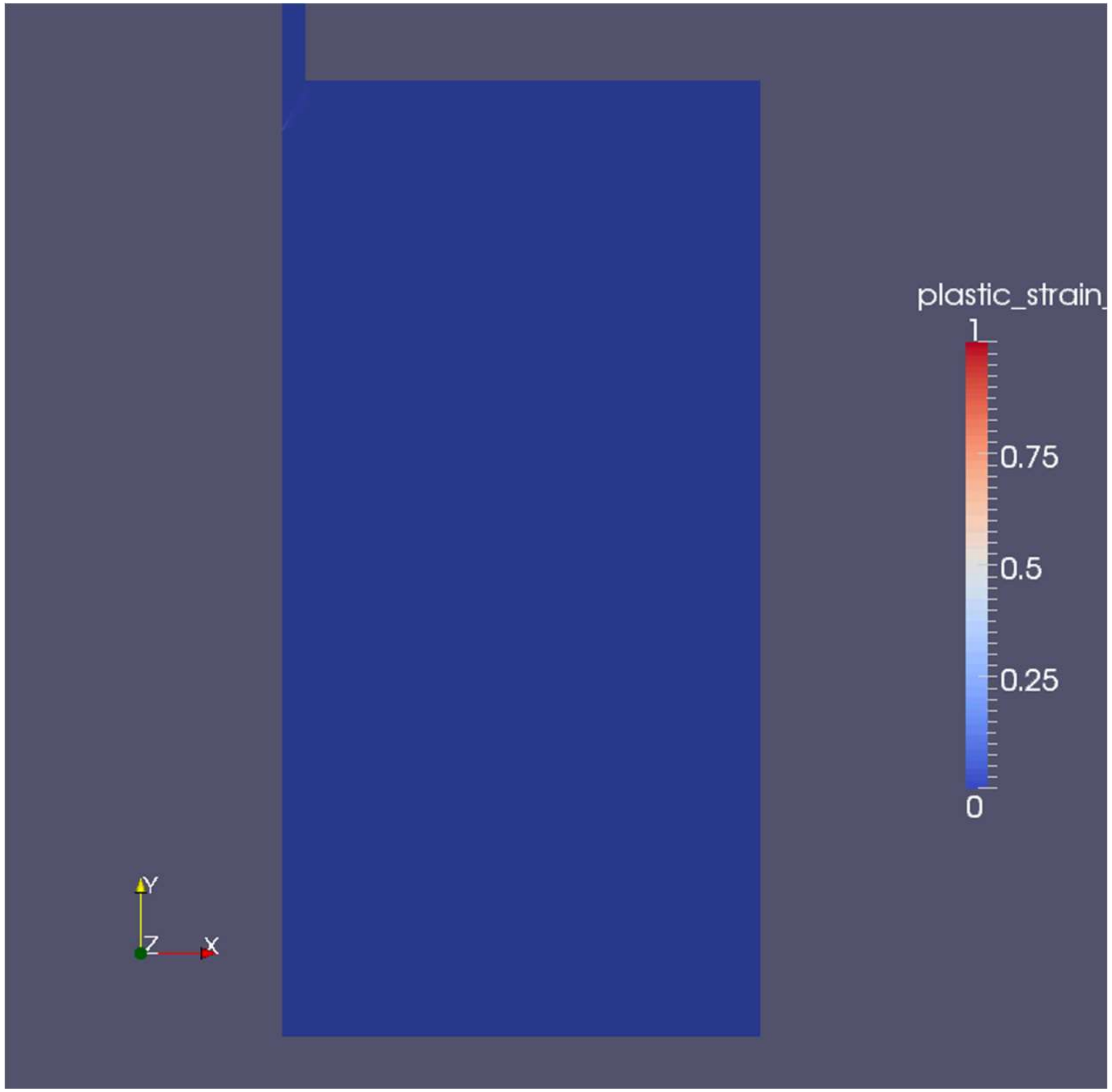

基于SPFEM的CPT解析

In undrained penetration, the cone resistance qc is commonly related to the undrained shear strength by way of a relation of the form

$$q_c = N_c c_u + \sigma_{v0}$$

where σ_{v0} is the total overburden stress (e.g. Teh & Houlsby, 1991; Lu et al., 2004)

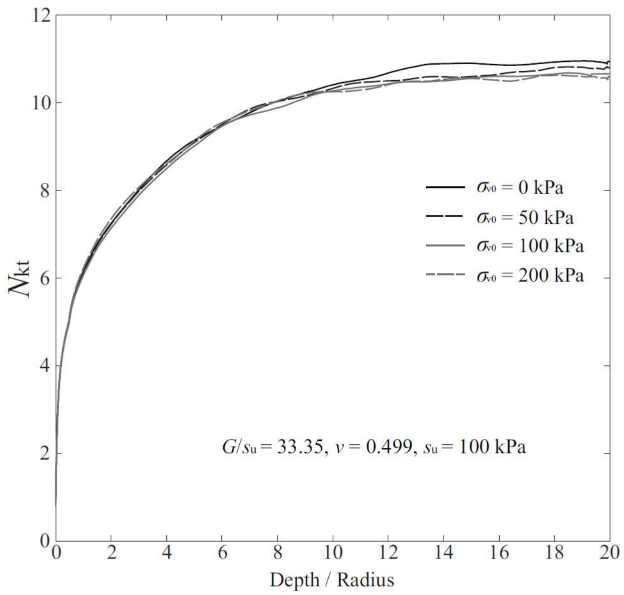

Figure 6: Cone factors versus overburden pressures

Cone factor with varying σ_{v0}

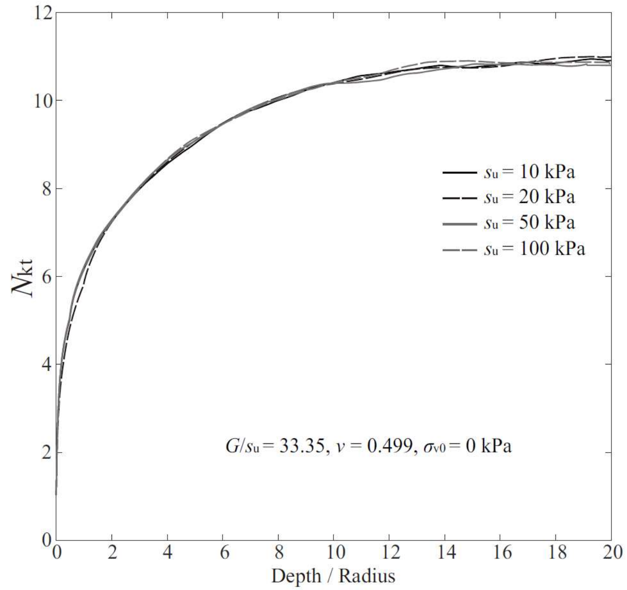

Cone factor with varying cu

Comparison against Existing Solutions

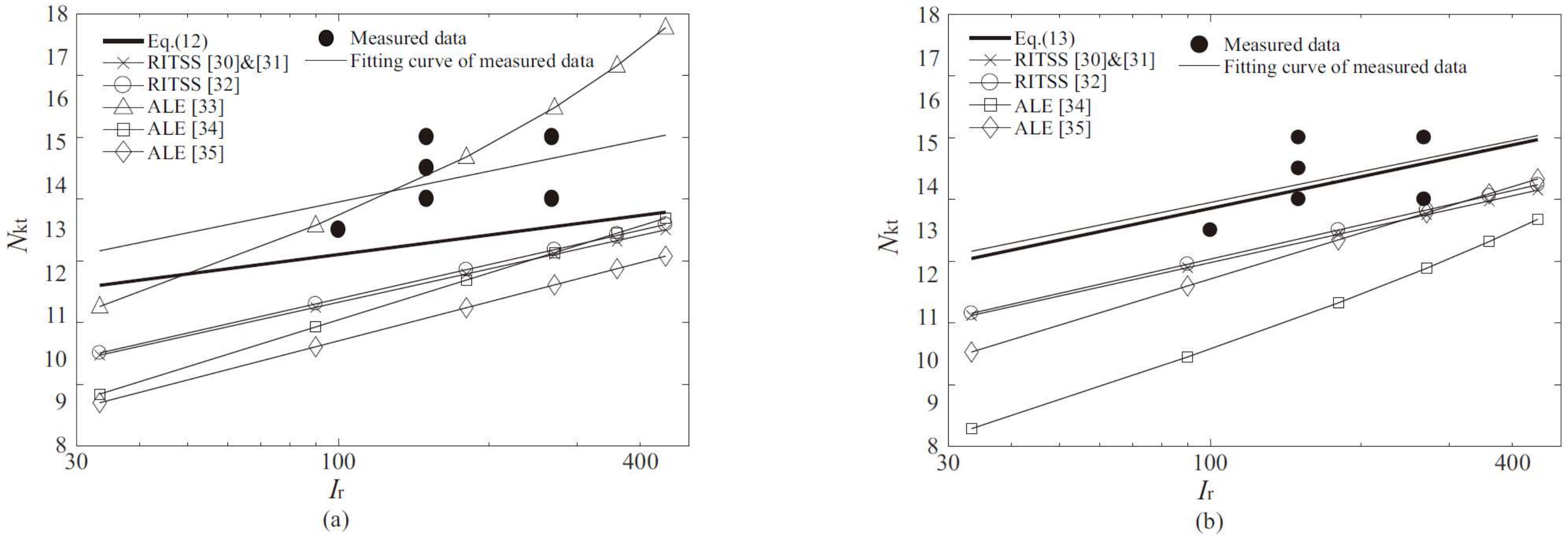

预制管桩贯入过程的模拟

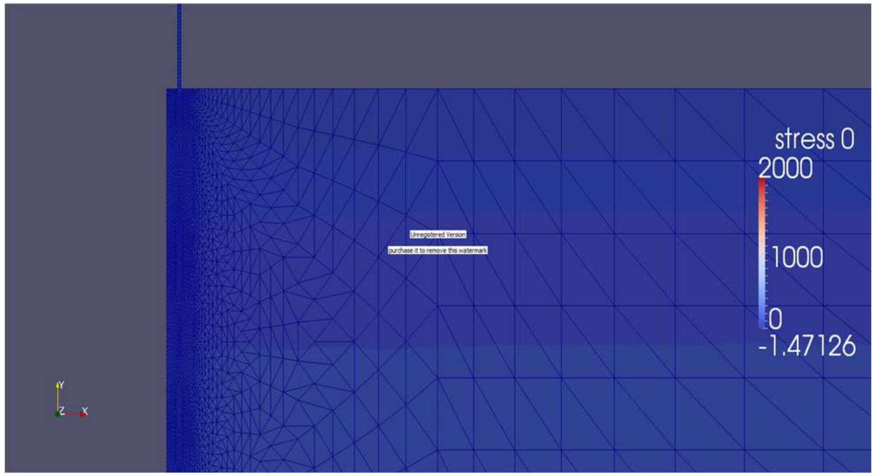

Radial stress σ_r

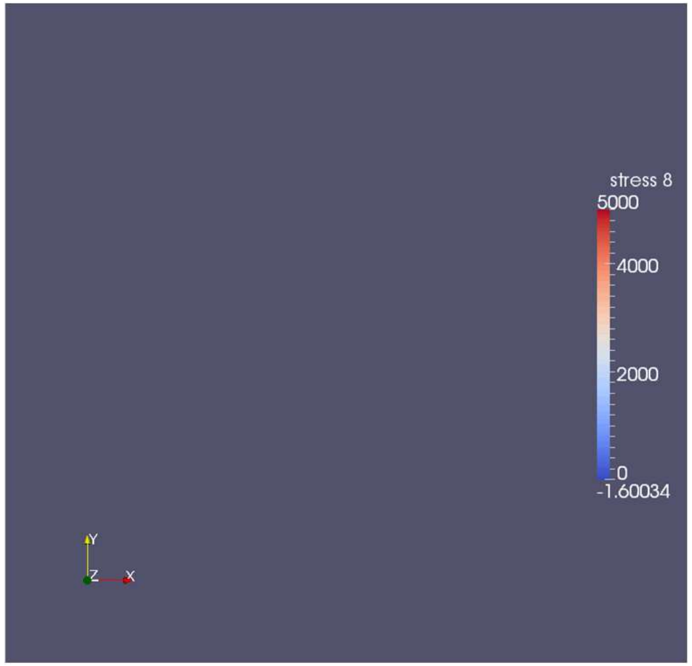

Vertical stress σ_z

Installation of an open-ended pile

相关文献

1. **Zhang W**, Yuan W, Dai B. Smoothed particle finite element method for large-deformation problems in geomechanics, International Journal of Geomechanics, 2018, 18(4): 04018010
2. Yuan W H, Wang B, **Zhang W**, et al. Development of an explicit smoothed particle finite element method for geotechnical applications. Computers and Geotechnics, 2019, 106: 42-51.
3. Yuan W, **Zhang W**(*), Dai B, Application of the particle finite element method for large deformation consolidation analysis, Engineering Computations, 2019, 36(9): 3138-3163
4. Yuan W, Liu K, **Zhang W**(*), et al. Dynamic modeling of large deformation slope failure using smoothed particle finite element method, Landslides, 2020, doi: 10.1007/s10346-020-01375-w
5. **Zhang W**, Zhong Z, Peng C, et al. GPU-accelerated smoothed particle finite element method for large deformation analysis in geomechanics. Computers & Geotechnics, doi: 10.1016/j.compgeo.2020.103856
6. YUAN Wei-Hai, WANG Hao-Cheng, **ZHANG Wei**(*), et al. Particle Finite Element Method implementation for large deformation analysis using Abaqus. Acta Geotechnica, 2021, doi: 10.1007/s11440-020-01124-2

报告人简介

张巍，华南农业大学水利与土木工程学院，副教授，硕士生导师。兼任中国土木工程学会土力学及岩土工程分会青年委员会委员、国际土力学学会会员。2010年博士毕业于武汉大学水利水电工程专业，2019年在维也纳自然资源与生命科学大学访学。主要研究方向为计算土力学、根加固土理论。针对岩土工程中常见的滑坡、泥石流等大变形问题，提出了岩土工程大变形数值模拟的光滑粒子有限元法(SPFEM)基本框架，并将其推广至动力与耦合分析，又进一步实现了三维GPU并行计算，为相关问题的研究提供了有效的数值工具。主持广东省自然科学基金1项、广东省水利科技创新项目1项、广州市荔湾区科技计划项目1项。共发表学术论文40余篇，其中SCI收录21篇（第一/通讯作者16篇）。成果主要发表在岩土工程国际著名期刊《Computers & Geotechnics》、《International Journal for numerical and analytical methods in geomechanics》、《Acta Geotechnica》、《International Journal of Geomechanics》、《Canadian Geotechnical Journal》、《Landslides》、《Bulletin of Engineering Geology and the Environment》等。获全国优秀水利水电工程勘测设计奖金质奖1项、广东省水利学会水利科学技术奖二等奖1项，授权发明专利2项，获软件著作权1项。

Email：zhangwei@scau.edu.cn 电话：13922426657